trisphosphate levels in drug-free schizophrenic patients. Psychiatry Research 118, 165–174.

Bauer, M., Maschberger, P., Quek, L., Briddon, S.J., Dash, D., Weiss, M., Watson, S.P., Siess, W., 2001. Genetic and pharmacological analyses of involvement of Src-family, Syk and Btk tyrosine kinases in platelet shape change. Src-kinases mediate integrin alphaIIb beta3 inside-out signalling during shape change. Thrombosis and Haemostasis 85, 331–340.

Benes, F.M., Vincent, S.L., Todtenkopf, M., 2001. The density of pyramidal and nonpyramidal neurons in anterior cingulate cortex of schizophrenic and bipolar subjects. Biological Psychiatry 50, 395–406.

Braff, D.L., Freedman, R., Schork, N.J., Gottesman, I.I., 2007. Deconstructing schizophrenia: an overview of the use of endophenotypes in order to understand a complex disorder. Schizophrenia Bulletin 33, 21–32.

Brickell, P.M., 1992. The p60c-src family of protein-tyrosine kinases: structure, regulation, and function. Critical Reviews in Oncogenesis 3, 401–446.

Cao, Q., Martinez, M., Zhang, J., Sanders, A.R., Badner, J.A., Cravchik, A., Markey, C.J., Beshah, E., Guroff, J.J., Maxwell, M.E., Kazuba, D.M., Whiten, R., Goldin, L.R., Gershon, E.S., Gejman, P.V., 1997. Suggestive evidence for a schizophrenia susceptibility locus on chromosome 6q and a confirmation in an independent series of pedigrees. Genomics 43, 1–8.

Casanova, M.F., Rothberg, B., 2002. Shape distortion of the hippocampus: a possible explanation of the pyramidal cell disarray reported in schizophrenia. Schizophrenia Research 55, 19–24.

Conrad, A.J., Abebe, T., Austin, R., Forsythe, S., Scheibel, A.B., 1991. Hippocampal pyramidal cell disarray in schizophrenia as a bilateral phenomenon. Archives of General Psychiatry 48, 413–417.

Crosby, D., Poole, A.W., 2003. Physical and functional interaction between protein kinase C delta and Fyn tyrosine kinase in human platelets. The Journal of Biological Chemistry 278, 24533–24541.

Davis, K.L., Stewart, D.G., Friedman, J.I., Buchsbaum, M., Harvey, P.D., Hof, P.R., Buxbaum, J., Haroutunian, V., 2003. White matter changes in schizophrenia: evidence for myelin-related dysfunction. Archives of General Psychiatry 60, 443–456.

Dror, N., Klein, E., Karry, R., Sheinkman, A., Kirsh, Z., Mazor, M., Tzukerman, M., Ben-Shachar, D., 2002. State-dependent alterations in mitochondrial complex I activity in platelets: a potential peripheral marker for schizophrenia. Molecular Psychiatry 7, 995–1001.

Ghosh, A.K., Reddi, A.L., Rao, N.L., Duan, L., Band, V., Band, H., 2004. Biochemical basis for the requirement of kinase activity for Cbl-dependent ubiquitinylation and degradation of a target tyrosine kinase. The Journal of Biological Chemistry 279, 36132–36141.

Goldsmith, J.F., Hall, C.G., Atkinson, T.P., 2002. Identification of an alternatively spliced isoform of the fyn tyrosine kinase. Biochemical and Biophysical Research Communications 298, 501–504.

Grant, S.G., O'Dell, T.J., Karl, K.A., Stein, P.L., Soriano, P., Kandel, E.R., 1992. Impaired long-term potentiation, spatial learning, and hippocampal development in fyn mutant mice. Science 258, 1903–1910.

Hattori, K., Uchino, S., Isosaka, T., Maekawa, M., Iyo, M., Sato, T., Kohsaka, S., Yagi, T., Yuasa, S., 2006. Fyn is required for haloperidol-induced catalepsy in mice. The Journal of Biological Chemistry 281, 7129–7135.

Hitchcock, I.S., Skerry, T.M., Howard, M.R., Genever, P.G., 2003. NMDA receptor-mediated regulation of human megakaryocytopoiesis. Blood 102, 1254–1259.

Ishiguro, H., Saito, T., Shibuya, H., Toru, M., Arinami, T., 2000. Mutation and association analysis of the Fyn kinase gene with alcoholism and schizophrenia. American Journal of Medical Genetics 96, 716–720.

Isosaka, T., Hattori, K., Yagi, T., 2006. NMDA-receptor proteins are upregulated in the hippocampus of postnatal heterozygous reeler mice. Brain Research 1073–1074, 11–19.

Kojima, N., Ishibashi, H., Obata, K., Kandel, E.R., 1998. Higher seizure susceptibility and enhanced tyrosine phosphorylation of *N*-methyl-D-aspartate receptor subunit 2B in fyn transgenic mice. Learning & Memory 5, 429–445.

Kovelman, J.A., Scheibel, A.B., 1986. Biological substrates of schizophrenia. Acta Neurologica Scandinavica 73, 1–32.

Levinson, D.F., Holmans, P., Straub, R.E., Owen, M.J., Wildenauer, D.B., Gejman, P.V., Pulver, A.E., Laurent, C., Kendler, K.S., Walsh, D., Norton, N., Williams, N.M., Schwab, S.G., Lerer, B., Mowry, B.J., Sanders, A.R., Antonarakis, S.E., Blouin, J.L., DeLeuze, J.F., Mallet, J., 2000. Multicenter linkage study of schizophrenia candidate regions on chromosomes 5q, 6q, 10p, and 13q: schizophrenia linkage collaborative group III. American Journal of Human Genetics 67, 652–663.

Lewis, C.M., Levinson, D.F., Wise, L.H., DeLisi, L.E., Straub, R.E., Hovatta, I., Williams, N.M., Schwab, S.G., Pulver, A.E., Faraone, S.V., Brzustowicz, L.M., Kaufmann, C.A., Garver, D.L., Gurling, H.M., Lindholm, E., Coon, H., Moises, H.W., Byerley, W., Shaw, S.H., Mesen, A., Sherrington, R., O'Neill, F.A., Walsh, D., Kendler, K.S., Ekelund, J., Paunio, T., Lonnqvist, J., Peltonen, L., O'Donovan, M.C., Owen, M.J., Wildenauer, D.B., Maier, W., Nestadt, G., Blouin, J.L., Antonarakis, S.E., Mowry, B.J., Silverman, J.M., Crowe, R.R., Cloninger, C.R., Tsuang, M.T., Malaspina, D., Harkavy-Friedman, J.M., Svrakic, D.M., Bassett, A.S., Holcomb, J., Kalsi, G., McQuillin, A., Brynjolfson, J., Sigmundsson, T., Petursson, H., Jazin, E., Zoega, T., Helgason, T., 2003. Genome scan meta-analysis of schizophrenia and bipolar disorder, part II: Schizophrenia. American Journal of Human Genetics 73, 34–48.

Li, S.S., 2005. Specificity and versatility of SH3 and other proline-recognition domains: structural basis and implications for cellular signal transduction. The Biochemical Journal 390, 641–653.

Lingjaerde, O., Kildemo, O., 1981. Dopamine uptake in platelets: two different low-affinity, saturable mechanisms. Agents Actions 11, 410–416.

Martinez, M., Goldin, L.R., Cao, Q., Zhang, J., Sanders, A.R., Nancarrow, D.J., Taylor, J.M., Levinson, D.F., Kirby, A., Crowe, R.R., Andreasen, N.C., Black, D.W., Silverman, J.M., Lennon, D.P., Nertney, D.A., Brown, D.M., Mowry, B.J., Gershon, E.S., Gejman, P.V., 1999. Follow-up study on a susceptibility locus for schizophrenia on chromosome 6q. American Journal of Medical Genetics 88, 337–343.

Martini, C., Tuscano, D., Trincavelli, M.L., Cerrai, E., Bianchi, M., Ciapparelli, A., Alessio, L., Novelli, L., Catena, M., Lucacchini, A., Cassano, G.B., Dell'Osso, L., 2006. Upregulation of A2A adenosine receptors in platelets from patients affected by bipolar disorders under treatment with typical antipsychotics. Journal of Psychiatric Research 40, 81–88.

Miller, A.L., Maas, J.W., Contreras, S., Seleshi, E., True, J.E., Bowden, C., Castiglioni, J., 1993. Acute effects of neuroleptics on unmedicated schizophrenic patients and controls. Biological Psychiatry 34, 178–187.

Miyakawa, T., Yagi, T., Kitazawa, H., Yasuda, M., Kawai, N., Tsuboi, K., Niki, H., 1997. Fyn-kinase as a determinant of ethanol sensitivity: relation to NMDA-receptor function. Science 278, 698–701.

Ohnuma, T., Kato, H., Arai, H., McKenna, P.J., Emson, P.C., 2003a. Expression of Fyn, a non-receptor tyrosine kinase in prefrontal cortex from patients with schizophrenia and its correlation with clinical onset. Brain Research. Molecular Brain Research 112, 90–94.

Ohnuma, T., Shibata, N., Matsubara, Y., Sato, S., Yamashina, M., Arai, H., 2003b. No genetic association between polymorphisms in the Fyn kinase gene and age of schizophrenic onset. Neuroscience Letters 343, 70–72.

Pagani, F., Baralle, F.E., 2004. Genomic variants in exons and introns: identifying the splicing spoilers. Nature reviews. Genetics 5, 389–396.

Plein, H., Berk, M., 2001. The platelet as a peripheral marker in psychiatric illness. Human Psychopharmacology 16, 229–236.

Rybakowski, J.K., Borkowska, A., Skibinska, M., Hauser, J., 2007. Polymorphisms of the Fyn kinase gene and a performance on the Wisconsin Card Sorting Test in schizophrenia. Psychiatric Genetics 17, 201–204.

Salter, M.W., Kalia, L.V., 2004. Src kinases: a hub for NMDA receptor regulation. Nature Reviews. Neuroscience 5, 317–328.

Schraw, T.D., Rutledge, T.W., Crawford, G.L., Bernstein, A.M., Kalen, A.L., Pessin, J.E., Whiteheart, S.W., 2003. Granule stores from cellubrevin/VAMP-3 null mouse platelets exhibit normal stimulus-induced release. Blood 102, 1716–1722.

Selemon, L.D., Rajkowska, G., Goldman-Rakic, P.S., 1998. Elevated neuronal density in prefrontal area 46 in brains from schizophrenic patients: application of a three-dimensional, stereologic counting method. The Journal of Comparative Neurology 392, 402–412.

Sperber, B.R., Boyle-Walsh, E.A., Engleka, M.J., Gadue, P., Peterson, A.C., Stein, P.L., Scherer, S.S., McMorris, F.A., 2001. A unique role for Fyn in CNS myelination. The Journal of Neuroscience 21, 2039–2047.

Tardito, D., Tura, G.B., Bocchio, L., Bignotti, S., Pioli, R., Racagni, G., Perez, J., 2000. Abnormal levels of cAMP-dependent protein kinase regulatory subunits in platelets from schizophrenic patients. Neuropsychopharmacology 23, 216–219.

Thakore, J.H., Walsh, M.T., Ryan, M., Hillmann, A., Condren, R., Kenny, D., Dinan, T., 2002. Elevated expression of integrin alpha (IIb) beta(IIIa) in drug-naive, first-episode schizophrenic patients. Biological Psychiatry 52, 874–879.

Tkachev, D., Mimmack, M.L., Ryan, M.M., Wayland, M., Freeman, T., Jones, P.B., Starkey, M., Webster, M.J., Yolken, R.H., Bahn, S., 2003. Oligodendrocyte dysfunction in schizophrenia and bipolar disorder. Lancet 362, 798–805.

Ventura, J., Lukoff, D., Nuechterlein, K.H., Liberman, R.P., Green, M.F., Shaner, A., 1993. Brief Psychiatric Rating Scale (BPRS) expanded version (4.0): Scales, anchor points, and administration manual. International Journal of Methods in Psychiatric Research 3, 227–243.

Weil, R., Levraud, J.P., Dodon, M.D., Bessia, C., Hazan, U., Kourilsky, P., Israel, A., 1999. Altered expression of tyrosine kinases of the Src and Syk families in human T-cell leukemia virus type 1-infected T-cell lines. Journal of Virology 73, 3709–3717.

Wittmann, M., Marino, M.J., Henze, D.A., Seabrook, G.R., Conn, P.J., 2005. Clozapine potentiation of N-methyl-D-aspartate receptor currents in the nucleus accumbens: role of NR2B and protein kinase A/Src kinases. The Journal of Pharmacology and Experimental Therapeutics 313, 594–603.

Yagi, T., 1999. Molecular mechanisms of Fyn-tyrosine kinase for regulating mammalian behaviors and ethanol sensitivity. Biochemical Pharmacology 57, 845–850.

Yasunaga, M., Yagi, T., Hanzawa, N., Yasuda, M., Yamanashi, Y., Yamamoto, T., Aizawa, S., Miyauchi, Y., Nishikawa, S., 1996. Involvement of Fyn tyrosine kinase in progression of cytokinesis of B lymphocyte progenitor. The Journal of Cell Biology 132, 91–99.

Yuasa, S., Hattori, K., Yagi, T., 2004. Defective neocortical development in Fyn-tyrosine-kinase-deficient mice. Neuroreport 15, 819–822.

Hippocampal Fyn activity regulates extinction of contextual fear

Tomoko Isosaka[a], Satoshi Kida[b], Tomoko Kohno[a], Kotaro Hattori[a] and Shigeki Yuasa[a]

Contextual fear memory is attenuated by reexposure of animals to a context alone without pairing it with an unconditioned stimulus, a phenomenon referred to as fear extinction. Here, we report that Fyn tyrosine kinase in the hippocampus is involved in the extinction of contextual fear. We inhibited Src-family tyrosine kinases in the dorsal hippocampus by stereotaxic injection of an inhibitor, PP2, and observed facilitation of extinction. We then biochemically analyzed dorsal hippocampal tissue during extinction training, and found that activated Fyn was significantly downregulated among the Src-family tyrosine kinases examined. These findings suggest that downregulation of Fyn activity facilitates the extinction of contextual fear. *NeuroReport* **20:1461–1465 © 2009 Wolters Kluwer Health | Lippincott Williams & Wilkins.**

NeuroReport 2009, **20**:1461–1465

Keywords: contextual fear conditioning, extinction, Fyn, hippocampus

[a]Department of Ultrastructural Research, National Institute of Neuroscience, National Center of Neurology and Psychiatry and [b]Department of Bioscience, Tokyo University of Agriculture, Tokyo, Japan

Correspondence to Dr Shigeki Yuasa, Department of Ultrastructural Research, National Institute of Neuroscience, National Center of Neurology and Psychiatry, 4-1-1 Ogawahigashimachi, Kodaira, Tokyo 187-8502, Japan
Tel: +81 42 346 1719; fax: +81 42 346 1749; e-mail: yuasa-s@ncnp.go.jp

Received 28 June 2009 **accepted** 17 August 2009

Introduction

Contextual fear conditioning is modeled experimentally by pairing placement of an animal in a training cage with a mild foot shock, so that the animal associates the context with the shock. Contextual memory can be measured by the increased freezing behavior, that is, elicited by reexposure to the context [1]. In contrast, if the animal is reexposed to the same context without pairing with foot shock, the freezing behavior eventually declines, a phenomenon referred to as 'extinction' of contextual fear memory [2,3].

A number of studies have shown that some, but not all, components of the molecular system that is required for the initial encoding of fear memory also regulate extinction [4,5]. We have previously reported finding that a member of the Src family of tyrosine kinases (SFKs), Fyn, plays a crucial role in memory formation in contextual fear conditioning, and that activation of the Fyn signaling pathway in the hippocampus is involved in the formation of contextual fear memory [6]. SFKs in the hippocampus have been reported to be involved in the extinction of fear-motivated memory based on a study that used the passive avoidance paradigm [7]. However, the significance of Fyn in fear memory extinction based on contextual fear conditioning remained to be elucidated.

In this study, we examined the effect of injection of PP2 (an SFK inhibitor [8]) into the hippocampus of mice on extinction of contextual fear memory, and we also examined the profile of hippocampal Fyn activation during the course of extinction training.

Materials and methods

Animals

Male C57BL/6J mice were purchased from Clea (Tokyo, Japan) and housed in the animal center of the institute under standard laboratory conditions as described earlier [9]. One week before the experiments, mice (12 to 13-week old) were housed individually and handled daily. All experiments were carried out in accordance with the guidelines of the United States National Institutes of Health (1996) and were approved by the Animal Care Committee of the National Institute of Neuroscience, National Center of Neurology and Psychiatry.

Drugs

4-Amino-5-(4-chlorophenyl)-7-(t-butyl) pyrazolo (3,4–D) pyrimidine (PP2) and 4-amino-7-phenylpyrazol (3,4–D) pyrimidine (PP3; inactive analog of PP2) were purchased from Calbiochem (San Diego, California, USA), dissolved in dimethyl sulfoxide, and brought to a final concentration of 25 μM with saline. The doses of PP2 and PP3 administered were based on the results of a pilot study and an earlier report [7].

Surgery and intrahippocampal injection

Mice were anesthetized with pentobarbital (50 mg/kg, intraperitoneally), and mounted on a stereotaxic apparatus (Narishige, Tokyo, Japan). Bilateral guide cannulae (Eicom, Kyoto, Japan) were implanted with their tips aimed at the dorsal hippocampus (anterior–posterior −2 mm, lateral ± 1.5 mm, depth 1.5 mm from the bregma). The guide cannulae were attached to the skull with dental cement, and dummy cannulae (Eicom) were inserted into the

DOI: 10.1097/WNR.0b013e32833203a8

guide cannulae during the experiments. PP2, PP3, or vehicle (0.25% dimethyl sulfoxide in saline), 0.8 μl per side was microinjected 1 week after surgery. The microinjections were performed at a rate of 0.4 μl/min through an injection cannula (Eicom) inserted through the guide cannula and connected through Teflon tubing to a microsyringe (Hamilton, Reno, Nevada, USA) driven by a microinfusion pump (Eicom). Cannula placement was verified by sectioning the brains (150 μM thick) coronally on a vibratome and visualizing the position of the track.

Contextual fear conditioning and extinction

The configuration of the context was as described earlier [6]. Contextual fear conditioning and extinction were carried out according to the procedure reported elsewhere [10], with slight modifications, as shown in Fig. 1a. On the day of the conditioning, the mouse was placed in the context and allowed 3 min 30 s to explore. A series of three foot shocks (0.6 mA, 125 V, 2 s) at 28 s intervals was then delivered, and 28 s later, the mouse was returned to its home cage. Extinction training was carried out 24 h after the conditioning. The hippocampus of the mice was injected with PP2, PP3, or vehicle and 10 min later the mice were reexposed to the context for 15 min without foot-shock pairing. One day after the extinction training, fear memory was assessed by measuring freezing time in the context for 5 min (Test). Freezing was defined as lack of any visible movement except respiration [12], and it was monitored by visual inspection of the video images without knowledge of the substance administered.

For the biochemical experiments, mice were conditioned as described above, and 24 h after conditioning, they were reexposed to the context alone for different times (0, 3, 15, or 30 min), and then immediately killed. The mice were designated Ext0, 3, 15, or 30, according to the duration of reexposure to the context alone. As shown in Fig. 2a, in the experiment to confirm the dependence of biochemical changes on extinction, a 'Context' mouse was placed in the context for 5 min without receiving any shocks, and 24 h later, the mouse was reexposed to the context for 30 min, and then immediately killed. A 'Shock' mouse received a series of three foot shocks at 28 s intervals immediately after being placed in the context, and was immediately returned to its home cage. Then, 24 h later, the mouse was reexposed to the context for 30 min, and immediately killed.

Antibodies

Antibodies against the Tyr418 of SFKs (pSrc418), Src, Yes, and Fyn were used in this study as described earlier [6].

Sample preparation and immunoblot analysis

For the immunoblotting studies, mice were killed by cervical dislocation, and hippocampal tissue, mainly consisting of the dorsal hippocampal area, was dissected out as described earlier [6]. The hippocampal tissue was then sonicated in sample buffer containing 1% SDS, 10 mM Tris pH 7.4, 1 mM sodium orthovanadate, and a protease inhibitor cocktail (Roche, Mannheim, Germany), and boiled at 95°C for 3 min. After centrifugation (4000*g*,

Fig. 1

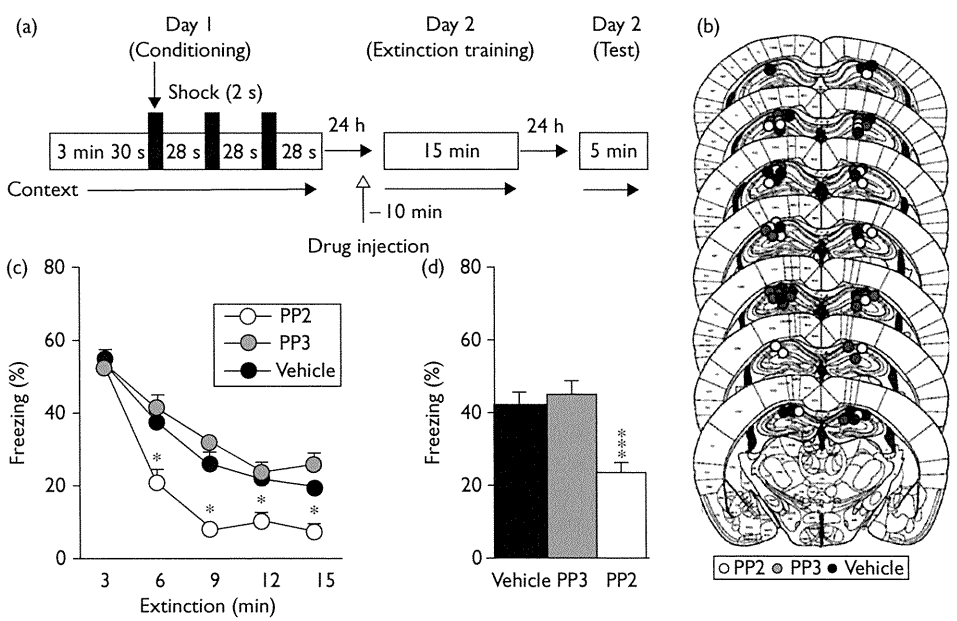

Effect of intrahippocampal injection of PP2 on contextual fear extinction. (a) Behavioral procedure. (b) Position of the tips of the guide cannulae in the hippocampus. Atlas templates were adapted from Paxinos and Franklin [11]. (c) Mean percentage freezing time averaged every 3 min during the extinction training. (d) Mean percentage freezing time during the 5 min test. $^{*}P<0.05$, $^{***}P<0.001$.

Fig. 2

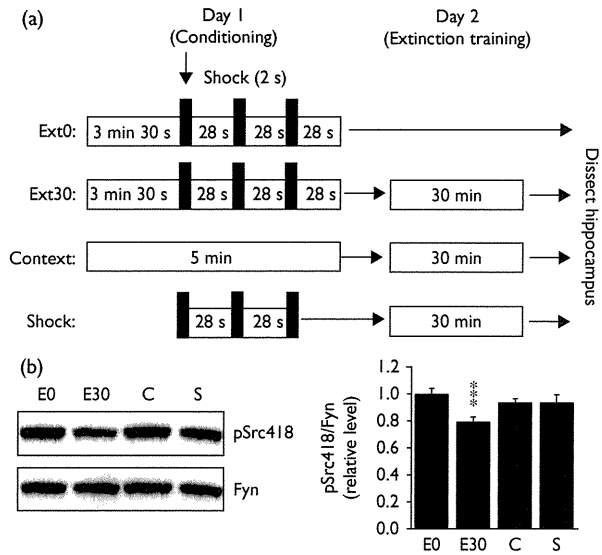

Downregulation of activated Fyn depends on extinction. (a) Behavioral procedure. (b) Western blot analysis of hippocampal tissue obtained from 'Ext0 (E0)', 'Ext30 (E30)', 'Context', and 'Shock' mice. The level of pSrc418 is shown as the density of pSrc418 normalized to the density of Fyn. The 'Ext0' level was set to 1.0. ***$P<0.001$. C, Context; S, Shock.

10 min), the supernatants were added to 4 × SDS sample buffer (50% glycerol, 125 mM Tris–HCl pH 6.8, 4% SDS, 0.08% bromophenol blue; Kinexus/*www.kinexus.ca*) and 40 mM dithiothreitol (Sigma, St. Louis, Missouri, USA), and boiled at 95°C for 2 min. An equal amount of lysate (10 µl per lane) was separated by SDS–polyacrylamide gel electrophoresis. The separated proteins were subsequently blotted onto Immobilon membranes (Millipore Co., Billerica, Massachusetts, USA), probed with each antibody, and visualized as described earlier [6].

Immunoprecipitation

Immunoprecipitation was performed as reported earlier [6] with slight modification. The sample buffer used in this study contained 50 mM Tris–HCl pH 8, 150 mM NaCl, 1% NP-40, 0.5% sodium deoxycholate, 0.1% SDS, 2 mM EDTA, 1 mM sodium orthovanadate, and a protease inhibitor cocktail (Roche).

Statistical analysis

All data are reported as means ± SEM. Student's *t*-test was used for pair-wise comparisons. One-way analysis of variance (ANOVA) or two-way repeated-measure ANOVA, followed by Tukey–Kramer test was used for biochemical or behavioral analysis as appropriate. *P* values less than 0.05 were considered statistically significant.

Results

To examine the effect of the SFK inhibitor on contextual fear extinction, the hippocampus of mice was implanted with a microcannula, and the mice were trained according to the behavioral schedule shown in Fig. 1a. Placement of the cannula tip for microinjection was almost identical across all groups of mice included in the analysis (Fig. 1b). During extinction training, the PP2 group ($n = 11$) exhibited significantly lower freezing levels than the vehicle group ($n = 12$) or PP3 group ($n = 11$), except during the initial 3-min extinction period (Fig. 1c). A two-way repeated-measure ANOVA with drug group (PP2, PP3, or vehicle) and extinction time (3, 6, 9, 12, and 15 min) as variables was performed on the freezing scores for extinction training, and the results showed a main effect of drug group [$F(2,31) = 12.773$, $P < 0.0001$], extinction time [$F(4,124) = 160.63$, $P < 0.0001$], and interaction [$F(8,124) = 5.5$, $P < 0.0001$]. Post-hoc Tukey–Kramer test showed significantly lower freezing levels in the PP2 group than in the vehicle group or PP3 group for each training time from 6 to 15 min ($P < 0.05$).

Next, we examined whether the extinction facilitated by the injection of PP2 before the extinction training was maintained for 24 h later. As shown in Fig. 1d, the freezing time during the test (5 min) was significantly lower in the PP2 group ($n = 11$) than in the vehicle group ($n = 12$) ($P < 0.001$). The freezing time in the PP3 group ($n = 11$) was unchanged in comparison with the vehicle group.

As shown in Fig. 1, inhibition of SFKs facilitated the extinction of contextual fear. However, as PP2 is not selective for any individual SFK, next we attempted to biochemically identify the SFK that was involved in the extinction. On the basis of the pilot study, we conducted stronger extinction training consisting of a 30 min reexposure to the context to identify clear differences between the SFKs. As shown in Fig. 3a, the mice reexposed to the context for 30 min (Ext30, $n = 12$) exhibited significantly lower freezing levels than the control mice (0 min reexposure; Ext0, $n = 12$) during the test ($P < 0.001$).

Next, we attempted to identify the SFK that exhibited a significant change after the extinction training. Hippocampal tissue was dissected immediately after training, and immunoprecipitation was performed with antibody against individual SFKs (Fyn, Src, and Yes). Thirteen to 14 animals were used in each group. Each immunoprecipitate was probed with the antibody against the phosphorylated Tyr418 residue of SFKs (pSrc418), because SFKs are activated by phosphorylation at Tyr418. As shown in Fig. 3b, the pSrc418 level in the immunoprecipitated Fyn ($P < 0.001$) and Src ($P < 0.01$) of the 'Ext30' group was significantly lower than in the 'Ext0' group. The immunoprecipitate with anti-pSrc418 was then probed with each SFK antibody. The amount of Fyn in the 'Ext30' immunoprecipitate was significantly lower than in the 'Ext0' immunoprecipitate ($P < 0.001$), and either Yes or Src was hardly detected in the anti-pSrc418 immunoprecipitate. On the basis of these

Fig. 3

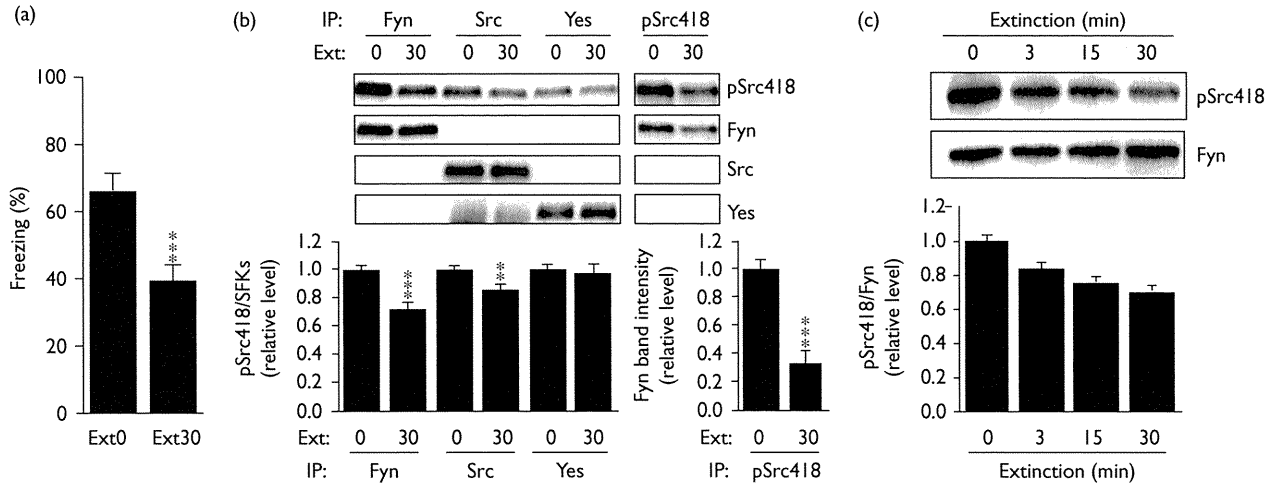

Activated Fyn in the hippocampus after extinction training. (a) Mean percentage freezing time during the 5 min test 1 day after extinction by reexposure to the context for 30 min. (b) Western blot analysis of each immunoprecipitated Src family of tyrosine kinase (SFK) protein. The panel on the left shows the density of pSrc418 normalized to that of immunoprecipitated Fyn, Src, and Yes, respectively. The panel on the right shows the density of Fyn in the immunoprecipitate by anti-pSrc418. (c) Western blot analysis of the hippocampal tissue during the course of extinction training. The level of pSrc418 is shown as the density of pSrc418 normalized to the density of Fyn. The level at 'Ext0' was set to 1.0. $^{**}P<0.01$, $^{***}P<0.001$. IP, immunoprecipitation.

findings, activated Fyn accounted for most of the activated SFK in the hippocampus, and for the most significant decrease after extinction training.

We then investigated the changes in activated Fyn during the course of extinction training by performing Western blotting of hippocampal tissue dissected immediately after extinction training for different times (3, 15, 30 min). Thirteen to 14 animals were used in each group. As shown in Fig. 3c, the pSrc418 level decreased during the course of extinction training. A one-way ANOVA of the pSrc418 level during extinction training showed a main effect of extinction time [$F(3,50) = 14.752$, $P < 0.0001$].

We also investigated whether the decrease in activated Fyn was dependent on the extinction of contextual fear memory by exposing mice to the behavioral procedure shown in Fig. 2a. Ten to 12 mice were used in each group. In this experiment, the 'Context' group was exposed to the context alone without pairing with a foot shock. The 'Shock' group received foot shocks immediately after being placed in the context. This procedure causes a defective association between the context and the shock, called 'immediate shock deficit' [13,14]. As shown in Fig. 2b, the pSrc418 level decreased significantly in the 'Ext30' group in comparison with the 'Ext0' group ($P < 0.001$). In contrast, the differences in pSrc418 levels in the 'Context' and 'Shock' group were not statistically significant from the level in the 'Ext0'group. This finding clearly confirms that the downregulation of activated SFKs, mostly activated Fyn, depends on fear memory extinction.

Discussion

The results of this study show that inhibition of hippocampal SFKs activity by PP2 facilitates extinction of contextual fear. In contrast, the level of activated Fyn in the hippocampus decreased significantly during the course of extinction training, and the decrease was dependent on the extinction of contextual fear memory. These results strongly suggest that downregulation of hippocampal Fyn activity facilitates the extinction of contextual fear memory.

Downregulation of cyclin-dependent kinase 5 (Cdk5) in the hippocampus has also been reported to facilitate extinction of contextual fear [15]. Fyn regulates Cdk5 activity through Tyr15 phosphorylation, and Fyn and Cdk5 are involved in the regulation of dendritic growth through the control of cytoskeletal reorganization [16]. Actin rearrangement and the subsequent alteration of synaptic structures in the hippocampus are now considered to be one of the mechanisms that underlie fear memory extinction [17]. Accordingly, both Fyn and Cdk5 in the hippocampus are presumed to be involved in the regulation of contextual fear extinction by crosstalk for synaptic remodeling through the cytoskeletal rearrangement.

We have reported earlier that activation of the Fyn signaling pathway in the hippocampus is required for acquisition of contextual fear memory [6], and the results of this study suggest that contextual fear extinction is regulated by counteracting the Fyn signaling pathway, and that mechanisms that downregulate activated Fyn might be involved in the process of extinction. The phosphatase activity of calcineurin in the amygdala has been reported

to be upregulated during extinction, and Akt, which is involved in fear memory acquisition, has been reported to be dephosphorylated [18]. Accordingly, any tyrosine phosphatase that dephosphorylates the activated Fyn may be an upstream regulator of Fyn in fear memory extinction. Further study will be necessary to identify the phosphatase that acts on the Fyn signaling pathway in extinction of contextual fear.

Conclusion

We showed that inhibition of SFK activity in the hippocampus facilitates extinction of contextual fear. Furthermore, among the SFKs investigated only activated Fyn was downregulated after extinction learning. These results strongly suggest that Fyn regulates extinction of contextual fear memory.

Acknowledgements

The authors are grateful to Dr M. Sekiguchi and D. Yamada (NCNP) for their instruction in the microinjection technique. This study was supported, in part, by the KAKENHI MEXT (18019044, 20019040) and by the NIBIO (grant 05–32).

References

1 LeDoux JE. Emotion circuits in the brain. *Annu Rev Neurosci* 2000; **23**:155–184.
2 Baum M. Spontaneous recovery from the effects of flooding (exposure) in animals. *Behav Res Ther* 1988; **26**:185–186.
3 Myers KM, Davis M. Behavioral and neural analysis of extinction. *Neuron* 2002; **36**:567–584.
4 Quirk GJ, Mueller D. Neural mechanisms of extinction learning and retrieval. *Neuropsychopharmacology* 2008; **33**:56–72.
5 Myers KM, Davis M. Mechanisms of fear extinction. *Mol Psychiatry* 2007; **12**:120–150.
6 Isosaka T, Hattori K, Kida S, Kohno T, Nakazawa T, Yamamoto T, *et al.* Activation of Fyn tyrosine kinase in the mouse dorsal hippocampus is essential for contextual fear conditioning. *Eur J Neurosci* 2008; **28**: 973–981.
7 Bevilaqua LR, da Silva WN, Medina JH, Izquierdo I, Cammarota M. Extinction and reaquisition of a fear-motivated memory require activity of the Src family of tyrosine kinases in the CA1 region of the hippocampus. *Pharmacol Biochem Behav* 2005; **81**:139–145.
8 Hanke JH, Gardner JP, Dow RL, Changelian PS, Brissette WH, Weringer EJ, *et al.* Discovery of a novel, potent, and Src family-selective tyrosine kinase inhibitor. Study of Lck- and FynT-dependent T cell activation. *J Biol Chem* 1996; **271**:695–701.
9 Hattori K, Uchino S, Isosaka T, Maekawa M, Iyo M, Sato T, *et al.* Fyn is required for haloperidol-induced catalepsy in mice. *J Biol Chem* 2006; **281**:7129–7135.
10 Suzuki A, Josselyn SA, Frankl PW, Masushige S, Silva AJ, Kida S. Memory reconsolidation and extinction have distinct temporal and biochemical signatures. *J Neurosci* 2004; **24**:4787–4795.
11 Paxinos G, Franklin K. *The mouse brain in stereotaxic coordinates.* New York: Academic Press; 2002.
12 Fanselow MS, Bolles RC. Naloxone and shock-elicited freezing in the rat. *J Comp Physiol Psychol* 1979; **93**:736–744.
13 Fanselow MS. Factors governing one-trial contextual conditioning. *Anim Learn Behav* 1990; **18**:264–270.
14 Landeira-Fernandez J, DeCola JP, Kim JJ, Fanselow MS. Immediate shock deficit in fear conditioning: effects of shock manipulations. *Behav Neurosci* 2006; **120**:873–879.
15 Sananbenesi F, Fischer A, Wang X, Schrick C, Neve R, Radulovic J, Tsai L. A hippocampal Cdk5 pathway regulates extinction of contextual fear. *Nat Neurosci* 2007; **10**:1012–1019.
16 Sasaki Y, Cheng C, Uchida Y, Nakajima O, Ohshima T, Yagi T, *et al.* Fyn and Cdk5 mediate semaphorin – a signaling, which is involved in regulation of dendrite orientation in cerebral cortex. *Neuron* 2002; **35**: 907–920.
17 Fischer A, Sananbenesi F, Schrick C, Spiess J, Radulovic J. Distinct roles of hippocampal de novo protein synthesis and actin rearrangement in extinction of contextual fear. *J Neurosci* 2004; **24**:1962–1966.
18 Lin CH, Yeh SH, Leu TH, Chang WC, Wang ST, Gean PW. Identification of calcineurin as a key signal in the extinction of fear memory. *J Neurosci* 2003; **23**:1574–1579.

Progress in Neuro-Psychopharmacology & Biological Psychiatry xxx (2011) xxx–xxx

Contents lists available at ScienceDirect

Progress in Neuro-Psychopharmacology & Biological Psychiatry

journal homepage: www.elsevier.com/locate/pnp

Expression of Ca^{2+}-dependent activator protein for secretion 2 is increased in the brains of schizophrenic patients

Kotaro Hattori [a,*], Haruko Tanaka [a], Chisato Wakabayashi [a], Noriko Yamamoto [a], Hirofumi Uchiyama [a], Toshiya Teraishi [a], Hiroaki Hori [a,b], Kunimasa Arima [c], Hiroshi Kunugi [a,b]

[a] Department of Mental Disorder Research, National Institute of Neuroscience, National Center of Neurology and Psychiatry, 4-1-1 Ogawahigashi-cho, Kodaira, Tokyo, 187-8502 Japan
[b] CREST, Japan Science and Technology Agency, 4-1-8 Honcho Kawaguchi, Saitama 332-0012, Japan
[c] Department of Psychiatry, National Center Hospital of Neurology and Psychiatry, National Center of Neurology and Psychiatry, 4-1-1 Ogawahigashi-cho, Kodaira, Tokyo, 187-8502 Japan

ARTICLE INFO

Article history:
Received 27 March 2011
Received in revised form 6 May 2011
Accepted 8 May 2011
Available online xxxx

Keywords:
BDNF
CAPS2
Postmortem brain
Schizophrenia
Stanley neuropathology consortium

ABSTRACT

Ca^{2+}-dependent activator protein for secretion 2 (CADPS2), a secretory granule associate protein, mediates monoamine transmission and the release of neurotrophins including brain-derived neurotrophic factor (BDNF) which have been implicated in psychiatric disorders. Furthermore, the expression of CADPS2deltaExon3, a defective splice variant of CADPS2, has been reported to be associated with autism. Based on these observations, we examined whether expression levels of CADPS2 and CADPS2deltaExon3 are altered in psychiatric disorders. Quantitative polymerase chain reaction analysis was performed for postmortem frontal cortex tissues (BA6) from 15 individuals with schizophrenia, 15 with bipolar disorder, 15 with major depression, and 15 controls (Stanley neuropathology consortium). The mean CADPS2 expression levels normalized to human glyceraldehyde-3phosphate dehydrogenase (GAPDH) or TATA-box binding protein levels was found to be significantly increased in the brains of the schizophrenia group, compared to the control group. On the other hand, the ratio of CADPS2deltaExon3 to total CADPS2 was similar in the 4 diagnostic groups. We then analyzed CADPS2 expression in blood samples from 121 patients with schizophrenia and 318 healthy controls; however, there was no significant difference between the two groups. Chronic risperidone treatment did not alter the expression of CADPS2 in frontal cortex of mice. The observed increase in the expression of CADPS2 may be related to the impaired synaptic function in schizophrenia.

1. Introduction

Ca^{2+}-dependent activator protein for secretion (CADPS) family, which consists of two members, CADPS1 and CADPS2, is a secretory granule-associated proteins involved in Ca^{2+}-dependent exocytosis of large dense-core vesicles containing diverse array of modulators including neurotrophines, monoamines and neuropeptides (Liu et al., 2008; Sadakata et al., 2004). CADPS2 mediates the release of neurotrophins such as brain-derived neurotrophic factor (BDNF) and neurotrophin-3. Mouse CADPS2 protein is associated with BDNF-containing secretory vesicles and promotes activity-dependent release of BDNF (Sadakata et al., 2004). BDNF release is significantly reduced in cultured neurons prepared from the brain of CADPS2 deficient mice (Sadakata et al., 2007a,b).

A number of findings suggest that BDNF action is impaired in psychiatric disorders including schizophrenia, bipolar disorder and depression. Several studies have shown decreased levels of BDNF or its receptor, TrkB, in the postmortem brains of patients with schizophrenia (Hashimoto et al., 2005; Iritani et al., 2003; Weickert et al., 2003), although there are contradictive reports (Chen et al., 2001; Dunham et al., 2009; Durany et al., 2001; Takahashi et al., 2000). The contribution of BDNF in depression has been suggested from animal studies that demonstrated stressful environments decrease, and antidepressive treatments increase BDNF levels in the brain (Duman and Monteggia, 2006; Martinowich et al., 2007). Also, centrally administered BDNF has an antidepressant-like effect in rat models (Siuciak et al., 1997). Thus, the molecules that contribute to the trafficking and release of BDNF may be a culprit of these disorders.

CADPS family also mediate monoamine transmission. Both CADPS1 and CADPS2 mediate the refilling of catecholamine to the releasable vesicles, and catecholamine secretion is significantly suppressed in the CADPS1/2 double deficient cells. (Liu et al., 2008). Another study supports that CADPS family are involved in monoamine storage as antibodies against CADPS1 or 2 inhibit monoamine

Abbreviations: ANCOVA, Analysis of covariance; BDNF, Brain-derived neurotrophic factor; CADPS2, Ca^{2+}-dependent activator protein for secretion 2; CCK, Cholecystokinin; DSM–IV, Diagnostic and Statistical Manual of Mental Disorders, 4th edition; FST, Freezer storage time; M.I.N.I., Mini-International Neuropsychiatric Interview; NT, Neurotensin; PCR, Polymerase chain reaction; PMI, Postmortem interval; SD, Standard deviation; TBP, TATA-box binding protein.

* Corresponding author at: 4-1-1 Ogawahigashi-cho, Kodaira, Tokyo, 187-8502, Japan. Tel.: +81 42 341 2712 Ex.5831; fax: +81 42 346 1744.
E-mail address: hattori@ncnp.go.jp (K. Hattori).

0278-5846/$ – see front matter © 2011 Elsevier Inc. All rights reserved.
doi:10.1016/j.pnpbp.2011.05.004

sequestration by synaptic vesicles from mice brain (Brunk et al., 2009).

Dysregulation of monoamine neurotransmission has been hypothesized to play a central role in the etiology of psychiatric disorders including schizophrenia and mood disorders. In schizophrenia, not only classical evidence that dopamine agonists induce and dopamine D2 receptor antagonists ameliorate psychoses but also brain imaging studies on drug naïve patients have suggested that dopamine transmission is affected in this disorder (Lyon et al., 2011). In major depression, reduced monoamine transmission hypothesis was derived from the finding that most anti-depressants increase monoamine levels in the synaptic cleft and that reserpine, a monoamine-depleting drug, worsen depressive symptoms in a subset of patients with mood disorder (Krishnan and Nestler, 2008), although imaging, postmortem, or cerebrospinal fluid studies have yet to find the definitive evidence for altered monoamine neurotransmission in this disorder (Belmaker and Agam, 2008; Nikolaus et al., 2009).

While, to our knowledge, CADPS2 expression in schizophrenia or mood disorders have not yet been examined, aberrant splicing of CADPS2 mRNA was reported in autism (Sadakata et al., 2007b). In this study, an exon-3 skipped isoform, CADPS2ΔExon3, was detected in the bloods of several autistic patients but not in those of healthy controls. They also showed that CADPS2ΔExon3 was deficient in proper axonal transport, which results in the loss of local synaptic BDNF release. Though the CADPS2ΔExon3 expression in the brains of patients with autism is unclear, the aberrant splicing of CADPS2 could contribute to susceptibility to autism by affecting neurotrophin release.

Based on above findings, the present study was aimed to examine whether the expression of CADPS2 transcripts is altered in the frontal cortex of patients with psychiatric disorders including schizophrenia, major depression and bipolar disorder. The CADPS2 expression levels in the blood of schizophrenia were also examined.

2. Materials and methods

2.1. Brain samples

Frozen postmortem samples of frontal cortex (BA6) were obtained from the Stanley Foundation Neuropathology Consortium (Torrey et al., 2000). The collection consists of 60 subjects: 15 with schizophrenia, 15 bipolar disorder, 15 major depression and 15 unaffected controls. All groups were matched for age, sex, race, pH and hemispheric side (Table 1), although postmortem interval (PMI) and freezer storage time differed across the groups. The brain tissues obtained were coded. Once our blind study was complete, we sent the data to the Stanley Foundation who then returned the codes, demographic and clinical data. In a cold-room, each frozen brain tissue was broken into powder in the plastic bag using dry-ice block and dry-ice-cold hammer. The powder was then transferred and kept in dry-ice-cold tubes. Temperature of the tubes and instruments that directly contacted to the samples was frequently measured by infrared–thermometer (AD-5613A, A&D Company, Japan) and kept under −20 °C. Then, 30 to 40 mg of brain powder was used for cDNA synthesis. RNA was extracted using RNAqueous (Applied biosystems, Foster City, CA) according to manufacturer's instructions with a slight modification, i.e., after homogenization, samples were washed twice with 500 μl of chloroform, and then applied to the spin-column. Extracted RNA was quantified by optical density reading at 260 nm using NanoDrop ND-1000 (Thermo Scientific, Rockford, IL). Then, the obtained RNA (14 μl) was used for cDNA synthesis using SuperScript VILO cDNA Synthesis Kit (Invitrogen, Carlsbad, CA).

Table 1
Demographic information on brain specimens of Stanley Neuropathology Consortium.

	Control	Schizophrenia	Bipolar disorder	Major depression
Age (years)	48.1 (29–68)	44.2 (25–62)	42.3 (25–61)	46.4 (30–65)
Gender (M/F)	9/6	9/6	9/6	9/6
Race	14 C, 1 AA	13 C, 2 A	14 C, 1 AA	15 C
PMI (hours)	23.7 (8–42)	33.7 (12–61)	32.5 (13–62)	27.5 (7–47)
pH	6.3 (5.8–6.6)	6.1 (5.8–6.6)	6.2 (5.8–6.5)	6.2 (5.6–6.5)
Side of brain frozen (R/L)	7/8	6/9	8/7	6/9
Freezer storage time (months)	11.3 (1–26)	20.7 (2–31)	20.7 (7–28)	14.5 (3–31)

AA, African American; A, Asian; C, Caucasian; F, female; M, male; and PMI, postmortem interval.

2.2. Blood samples

Subjects were 121 patients with schizophrenia (84 males and 37 females; age 44.1 ± 13.7 (mean ± SD) years) and 318 controls (90 males and 228 females; age 43.1 ± 15.3 years). All subjects were biologically unrelated Japanese and recruited from the same geographical area (Western part of Tokyo Metropolitan). Consensus diagnosis by at least two psychiatrists was made for each patient according to the Diagnostic and Statistical Manual of Mental Disorders, 4th edition (DSM–IV) criteria (American Psychiatric Association, 1994) on the basis of unstructured interviews and information from medical records. The controls were healthy volunteers recruited from the community, through advertisements in free local magazines and our website announcement. Control individuals were interviewed by the Japanese version of the Mini-International Neuropsychiatric Interview (M.I.N.I.) (Otsubo et al., 2005; Sheehan et al., 1998) and those who had a current or past history of psychiatric treatment were not enrolled in the study. After the nature of the study procedures had been fully explained, written informed consent was obtained from all subjects. The study was conducted in accordance with the Declaration of Helsinki and approved by the ethics committee of the National Center of Neurology and Psychiatry, Japan.

Blood collection and RNA isolation were performed using the PAXgene blood RNA system (Qiagen, Valencia, CA). Blood samples were collected around 11 A.M. Extracted RNA was quantified as described above. Samples that contained more than 40 ng/μl of total RNA were used for analysis; 8 μl from each sample was reverse transcribed using SuperScript VILO cDNA Synthesis Kit (Invitrogen, Carlsbad, CA).

2.3. Chronic risperidone treatment to mice

C57BL/6J male mice aged 10 weeks were purchased from Crea Japan. Chronic oral risperidone treatment was performed according to Belforte et al., (Belforte et al., 2010). In brief, 2.5 mg/kg/day of risperidone (Rispadal liquid, Janssen Pharmaceutical, Tokyo, Japan) in drinking water freshly made every 72 h had been administered continuously for 3 weeks. Control mice received solvent (1.4 mM tartaric acid neutralized to pH 6–7). All experimental procedures were in accordance with the guidelines of the United State's National Institutes of Health (1996) and were approved by the Animal Care Committee of the National Institute of Neuroscience, NCNP.

2.4. Quantitative real-time polymerase chain reaction

Polymerase chain reaction (PCR) amplifications were performed in triplicate (5 μl volume) on 384-well plates using ABI prism 7900HT (Applied Biosystems, Foster City, CA). Each reaction contained 0.28 μl of cDNA sample, qPCR QuickGoldStar Mastermix Plus (Eurogentec, Seraing, Belgium) and a primer of the target, i.e. human CADPS2 (Hs01095968_m1 at Exon 4–5 on NM_017954.9), mouse CADPS2 (Mm00462577_m1), human CADPS2ΔExon3 (Forward primer: GTAGCTGACGAAGCATTTTGCA,

Please cite this article as: Hattori K, et al., Expression of Ca^{2+}-dependent activator protein for secretion 2 is increased in the brains of schizophrenic patients, Prog Neuro-Psychopharmacol Biol Psychiatry (2011), doi:10.1016/j.pnpbp.2011.05.004

Reverse Primer: TGATCTGGGCTGCTTGTTCAT, Reporter: CTGCGTTATC-CAGCTCAT) and a primer of the housekeeping gene human glyceraldehyde-3phosphate dehydrogenase (GAPDH, 4326317E), mouse GAPDH (4352339E) and human TATA-box binding protein (TBP, Hs99999910_ml) all purchased from Applied Biosystems (Foster City, CA). Negative control reactions were carried out with "no RNA" samples. The real time PCR reactions ran at 50 °C for 2 min, at 95 °C for 10 min and in 40 or 45 cycles changing between 95 °C for 15 s and 60 °C for 1 min. A standard amplification curve was made by serial dilution of a "standard" pooled cDNA sample in each plate. The mean value of triplicate of each sample was normalized to the standard curve. Then, the values of CADPS2 and CADPS2ΔExon3 from each sample were normalized to those of GAPDH.

2.5. Statistical analyses

Data analyses were performed with SPSS software (Version 11, SPSS Japan, Tokyo, Japan). Effect of age, brain pH, postmortem interval (PMI), and freezer storage time on each brain analysis was assessed by Pearson's correlations (Table 2). Variables showing significant correlations were included as covariates in the main analysis. Levene's test was used to assess the equality of variances across diagnostic group. Analysis of covariance (ANCOVA) was used to identify overall effects of diagnosis and significant main effects of diagnosis were investigated by planned post hoc contrasts. In the blood sample analyses, CADPS2 expression levels were converted to 10-log scale before statistical analysis in order to obtain a normal distribution (Castensson et al., 2005). The effect of diagnosis on blood CADPS2 expression was assessed by ANCOVA with sex and age as covariates after Levene's test. The effect of diagnosis on blood CADPS2ΔExon3 expression was assessed by logistic regression, controlling for sex and age as covariates. The effect of risperidone on CADPS2 expression in mice brain was assessed by student's *t*-test after F-test.

3. Results

3.1. CADPS2 expression levels in the postmortem brain (BA6)

We first analyzed the effects of age, brain pH, postmortem interval (PMI), and freezer storage time (FST) on each expression analysis (Table 2). Brain pH was significantly correlated with GAPDH expression levels or raw CADPS2 expression levels. PMI also tended to be correlated with GAPDH expression levels or raw CADPS2 expression levels. If the effects were analyzed separately within each diagnostic group, no significant correlation was detected.

CADPS2 expression levels normalized to GAPDH expression levels (CADPS2/GAPDH) in each sample are shown in Fig. 1A. ANCOVA with brain pH as covariates detected a significant effect of diagnosis on CADPS2/GAPDH levels ($F=3.4$, $df=3$, $p=0.025$) and post hoc test detected a significant difference between schizophrenia and control groups ($p=0.03$). Even if PMI was added as another covariate, the difference was significant ($p=0.002$). There was no significant difference between bipolar disorder and controls or between depression and controls. There was no significant correlation between CADPS2/GAPDH levels and lifetime dose of antipsychotic drugs (data not shown). There was a significant effect of diagnosis on GAPDH expression levels ($F=3.4$, $df=3$, $p=0.023$, Fig. 1B). GAPDH levels in the control group was significantly higher than that of schizophrenia ($p=0.012$), bipolar disorder ($p=0.009$) or major depression group ($p=0.013$). Raw CADPS2 levels did not differ among the diagnostic groups ($F=1.0$, $df=3$, $p=0.38$, Fig. 1C). There was a significant correlation between GAPDH expression levels and raw CADPS2 expression levels (Pearson's correlation 0.69, $p<0.001$, Fig. 1D).

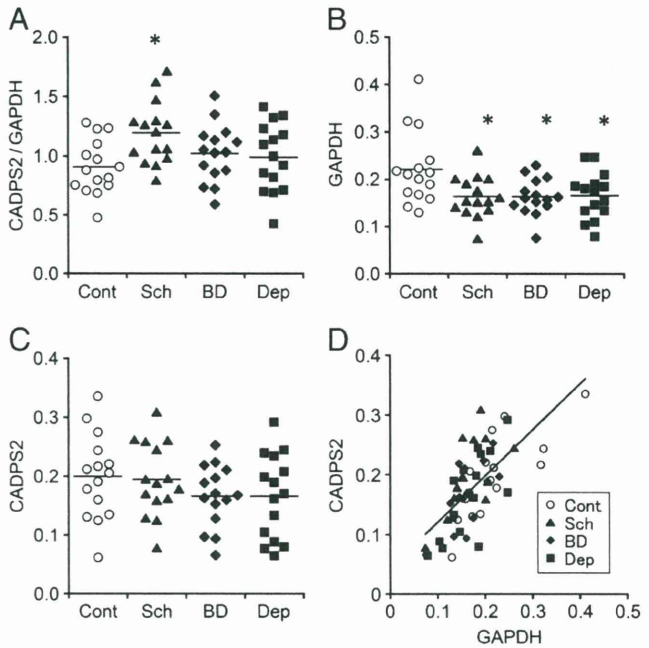

Fig. 1. CADPS2 expression levels in the postmortem brains of psychiatric disorder. (A) CADPS2 expression levels normalized by GAPDH levels. Scatter plots display the variability and differences in the CADPS2 mRNA expression levels normalized by each GAPDH expression levels. A crossbar on each scatter plot represents mean expression levels for each group. (B) GAPDH expression levels (C) Raw CADPS2 expression levels. (D) Correlation between GAPDH levels and raw CADPS2 levels. Cont, control; Sch, schizophrenia; BD, Bipolar Disorder; and Dep, Depression. *, statistically significant difference ($p<0.05$).

We compared relative CADPS2 expression levels among diagnostic groups using another endogenous control, TATA-box binding protein (TBP), and obtained similar result (Fig. S1, this experiment was done after uncode the sample). ANCOVA with brain pH as covariates detected a significant effect of diagnosis on CADPS2/TBPlevels ($F=3.3$, $df=3$, $p=0.027$) and post hoc test detected a significant

Table 2
The effect of age, pH, postmortem interval, and freezer storage time on each brain expression analysis.

		GAPDH	CADPS2	ΔExon3	CADPS2/GAPDH	ΔExon3/G APDH	ΔExon3/C ADPS2
Age	Pearson's	0.013	−0.13	0.19	−0.18	0.088	0.27
	P	0.92	0.34	0.37	0.16	0.51	0.041
pH	Pearson's	0.36	0.26	0.25	0.031	0.12	0.090
	p	0.005	0.048	0.058	0.81	0.38	0.50
Post mortem Pearson's interval (hours)	−0.23	−0.22	−0.13	−0.040	0.039	0.15	
	P	0.076	0.098	0.30	0.76	0.77	0.25
Freezer storage time (months)	Pearson's	−0.22	−0.034	−0.041	0.21	0.12	0.052
	P	0.092	0.80	0.75	0.11	0.36	0.69

ΔExon3, CADPS2ΔExon3; and Pearson's, Pearson's correlation.

Please cite this article as: Hattori K, et al., Expression of Ca^{2+}-dependent activator protein for secretion 2 is increased in the brains of schizophrenic patients, Prog Neuro-Psychopharmacol Biol Psychiatry (2011), doi:10.1016/j.pnpbp.2011.05.004

difference between schizophrenia and control groups ($p=0.019$). Even if PMI was added as another covariate, the difference was significant ($p=0.012$).

With respect to CADPS2ΔExon3/GAPDH level (Fig. 2A), the effect of age was detected in the control group (Pearson's correlation 0.58, $p=0.023$) and the effect of pH was detected in the bipolar disorder group (Pearson's correlation 0.60, $p=0.018$). ANCOVA with age and brain pH as covariates detected the marginal effect of diagnosis ($F=2.8$, $df=3$, $p=0.050$) and the mean expression level was significantly increased in the schizophrenia group, compared to the control group ($p=0.030$). When the ratio of CADPS2ΔExon3 to raw (total) CADPS2 expression levels was compared, the ratio was similar in the 4 diagnostic groups ($F=1.1$, $df=3$, $p=0.36$, Fig. 2B). Neither the effect of diagnosis on raw CADPS2ΔExon3 levels was observed ($F=1.9$, $df=3$, $p=0.15$, Fig. 2C). There was a significant correlation between GAPDH expression levels and raw CADPS2ΔExon3 expression levels (Pearson's correlation 0.66, $p<0.001$, Fig. 2D).

3.2. Cortical CADPS2 expression after chronic antipsychotic treatment in mice

To see whether antipsychotics alter the mRNA expression of CADPS2, we measured the CADPS2 levels in the frontal cortex of mice, following chronic treatment with an antipsychotic risperidone. Oral administration of risperidone (2.5 mg/kg, $n=15$ for the controls and 16 for the risperidone group) for 3 weeks did not alter CADPS2 expression ($F=1.5$, $df=29$, $p=0.61$).

3.3. CADPS2 expression in blood sample

Since we observed increased expression of CADPS2 in postmortem brains of schizophrenia patients, we then examined whether such an alteration exists in peripheral blood samples. The CADPS2/GAPDH expression levels were converted to 10-logarism before statistical analyses to obtain normal distribution. The mean (Standard deviation) CADPS2 expression level was 0.17 (1.29) in the control group and 0.32 (1.46) in the schizophrenia group. ANCOVA controlling for age and sex did not detect the significant effect of diagnosis on CADPS2/GAPDH level ($F=1.67$, $df=1$, $p=0.20$). We also measured CADPS2ΔExon3 levels in the blood samples. Compared to brain samples, the expression levels were quite low and could not detect in the majority of samples. Thus, we defined "expressed" when at least 2 tubes in triplet analyses of each sample were detected until 45 cycles. CADPS2ΔExon3 expression was detected in 36 of 318 control samples (ratio = 0.11), and 21 of 121 schizophrenia samples (ratio = 0.17). There was no significant effect of diagnosis on CADPS2ΔExon3 expression by the logistic regression analysis controlling for age and sex (odds ratio 1.51, [95% CI 0.80–2.86], $p=0.21$). Even when men and women were examined separately, there was no significant difference between the patients and controls for each sex (data not shown).

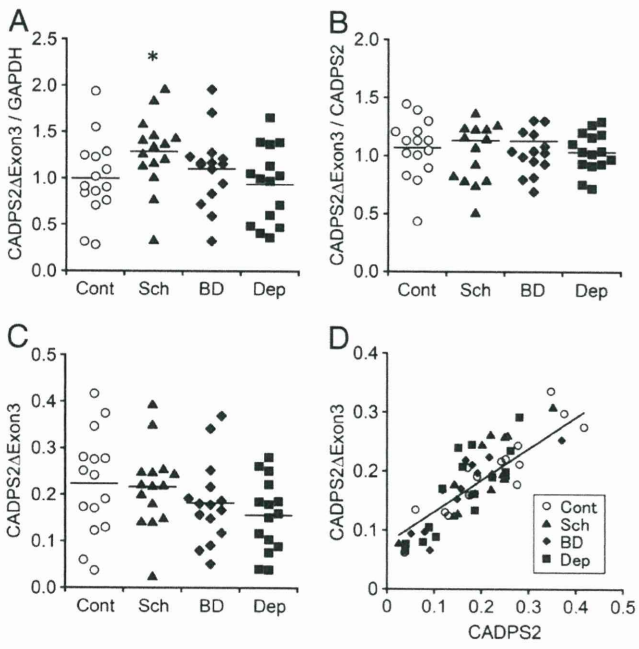

Fig. 2. CADPS2ΔExon3 expression levels in the postmortem brains of psychiatric disorder. (A) CADPS2ΔExon3 expression levels normalized by GAPDH levels. Scatter plots display the variability and differences in the CADPS2ΔExon3 mRNA expression levels normalized by each GAPDH expression levels. A crossbar on each scatter plot represents mean expression levels for each group. (B) CADPS2ΔExon3 levels normalized to each total CADPS2 expression levels. (C) Raw CADPS2ΔExon3 expression levels. (D) Correlation between GAPDH expression levels and raw CADPS2ΔExon3 expression levels. Cont, control; Sch, schizophrenia; BD, Bipolar Disorder; and Dep, Depression. *, statistically significant difference ($p<0.05$).

4. Discussion

4.1. Main findings

In the present study, we analyzed the expression of CADPS2 mRNA in the postmortem brains (BA6) of psychiatric patients (schizophrenia, major depression and bipolar disorder) and controls. A significant increase in the CADPS2 expression was detected in the brains of the schizophrenia group, compared to the control group. No change was detected in other disease groups. While a CADPS2 splice variant, CADPS2ΔExon3 showed a non-significant increase in the schizophrenia group, its ratio to the total CADPS2 levels was not different from the control group. Chronic risperidone treatment did not alter the CADPS2 levels in mice brain. We also analyzed CADPS2 or CADPS2-ΔExon3 expression levels in the blood samples of schizophrenia and control subjects; however, the levels were not significantly different between the two groups.

4.2. Brain analysis

4.2.1. Drug effect

A large number of gene expressions in the brain are affected by antipsychotic treatments (Girgenti et al.,; Mehler-Wex et al., 2006; Thomas, 2006). Therefore, the observed increase in CADPS2 mRNA in the schizophrenia group could be the result of antipsychotic treatment. However, our results did not support this assumption because the CADPS2 levels did not correlate to life-time antipsychotic dose and chronic risperidone treatment in mice did not alter CADPS2 expression on their cortices, although caution is required for the interpretation of those results because we don't have data for the latest dose before death and other drugs such as chlorpromazine, haloperidol and clozapine might be used in the patients.

4.2.2. Possible relevance to BDNF secretion, dopamine transmission, and neuropeptide release

Considering that defective BDNF signaling has been suggested in schizophrenia and mood disorders (Angelucci et al., 2005) and that CADPS2 mediates BDNF release in neurons (Sadakata et al., 2004), we initially expected that CADPS2 levels would be decreased in frontal cortex in patients with these psychiatric disorders. However, in our results, CADPS2 levels were not altered in mood disorders but increased in schizophrenia. In addition, the relative levels of defective CADPS2 isoform, CADPS2ΔExon3 were not altered in those disorders. Thus, it is unlikely that altered CADPS2 expression might be a cause of BDNF deficits in schizophrenia. It may be rather a compensatory consequence of reduced BDNF signaling.

Please cite this article as: Hattori K, et al., Expression of Ca^{2+}-dependent activator protein for secretion 2 is increased in the brains of schizophrenic patients, Prog Neuro-Psychopharmacol Biol Psychiatry (2011), doi:10.1016/j.pnpbp.2011.05.004

CADPS2 also promotes monoamine storage in neurons (Brunk et al., 2009; Liu et al., 2008). CADPS2 is highly expressed in the dopamine-rich brain areas such as ventral tegmental area and substantia nigra of mice brain (Sadakata et al., 2006) and it is reported to interact with dopamine D2 receptor (Binda et al., 2005). Growing evidence has demonstrated increased presynaptic dopamine levels in the striatum of schizophrenia patients (Lyon et al., 2009). If the observed increase in the expression of CADPS2 occurs in the subcortical regions including striatum and midbrain as well as frontal cortex, it might be the cause of hyper-dopamine transmission that reflects psychotic state (Howes et al., 2009).

Furthermore, large dense-core vesicles contain not only neurotrophins and monoamines but also neuropeptides (Salio et al., 2006). Neuropeptides such as endorphins, cholecystokinin (CCK), neurotensin (NT), somatostatin, Neuropeptide Y and neuregulin 1 have been implicated in schizophrenia (Caceda et al., 2007). Especially reduced levels of CCK and NT have been repeatedly reported in the disorder (Caceda et al., 2007), which may have caused compensatory increase in the CADPS2 expression in schizophrenia.

4.3. CADPS2 expression in the blood

4.3.1. CADPS2 expression and diagnosis

Following the report that 4 of 16 patients with autism expressed CADPS2ΔExon3 in peripheral bloods but none in 24 normal subjects (Sadakata et al., 2007b), another group reported that they detected CADPS2ΔExon3 in some control subjects (Eran et al., 2009). Thus we assumed that the ratio of CADPS2ΔExon3 to total CADPS2 rather than whether CADPS2ΔExon3 exists or not is important and therefore we applied quantitative real-time PCR to measure their expression. The pilot experiment in the present study indicated that our quantification method using SuperScript VILO and random-hexamer, was 4 to 8 fold more sensitive than one step real-time PCR using gene specific primers and could detect l0 to 100 clones of CADPS2 or CADPS2-ΔExon3 sequence-containing vector. Compared with the brains, CADPS2 expression was 32 to 128 fold lower in the blood. Unlike in the brain, CADPS2ΔExon3 could not be detected in most blood samples. So we performed qualitative analysis for each subject. As a result, we didn't detect any significant difference in the expression of CADPS2ΔExon3 in the blood between patients with schizophrenia and controls. The CADPS2ΔExon3 was abundantly expressed in the brain and the levels were unchanged across the diagnostic groups. Thus, it is unlikely that the expression or the splicing balance should relate to diseases we analyzed.

5. Conclusion

In conclusion, we found increased mRNA expression of CADPS2 in the postmortem frontal cortex of schizophrenia patients which might have some relevance to dysregulation in the release of dopamine, neurotrophins, and/or neuropeptides in the disorder. This increase was unlikely to be attributable to antipsychotic medication. We also analyzed the CADPS2ΔExon3 in human brains and found that it is abundantly present in the frontal cortex in any diagnostic group. We obtained no evidence for the specific role of the splice variant in schizophrenia or mood disorders. Future research should include the evaluation of CADPS2 expression in other brain areas, and basic studies on the cause and consequence of increased CADPS2 expression.

Supplementary materials related to this article can be found online at doi:10.1016/j.pnpbp.2011.05.004.

Acknowledgments

Postmortem brain tissue was donated by The Stanley Medical Research Institute's brain collection courtesy of Drs. Michael B. Knable, E. Fuller Torrey, Maree J. Webster, and Robert H. Yolken. We thank Dr. Teiichi Furuichi for helpful comments to the manuscript. This work was supported by a Health and Labor Science Research Grant (H21-KOKORO-WAKATE-20; H21-KOKORO-001), CREST of JST, Grant-in-Aid for Scientific Research (KAKENHI, 22591269), Intramural Research Grant for Neurological and Psychiatric Disorders of NCNP, Takeda Science Foundation, and Mitsubishi Pharma Research Foundation.

References

Angelucci F, Brene S, Mathe AA. BDNF in schizophrenia, depression and corresponding animal models. Mol Psychiatry 2005;10:345–52.
Belforte JE, Zsiros V, Sklar ER, Jiang Z, Yu G, Li Y, et al. Postnatal NMDA receptor ablation in corticolimbic interneurons confers schizophrenia-like phenotypes. Nat Neurosci 2010;13:76–83.
Belmaker RH, Agam G. Major depressive disorder. N Engl J Med 2008;358:55–68.
Binda AV, Kabbani N, Levenson R. Regulation of dense core vesicle release from PC12 cells by interaction between the D2 dopamine receptor and calcium-dependent activator protein for secretion (CAPS). Biochem Pharmacol 2005;69:1451–61.
Brunk I, Blex C, Speidel D, Brose N, Ahnert-Hilger G. Ca^{2+}-dependent activator proteins of secretion promote vesicular monoamine uptake. J Biol Chem 2009;284:1050–6.
Caceda R, Kinkead B, Nemeroff CB. Involvement of neuropeptide systems in schizophrenia: human studies. Int Rev Neurobiol 2007;78:327–76.
Castensson A, Aberg K, McCarthy S, Saetre P, Andersson B, Jazin E. Serotonin receptor 2C (HTR2C) and schizophrenia: examination of possible medication and genetic influences on expression levels. Am J Med Genet B Neuropsychiatr Genet 2005;134B:84–9.
Chen B, Dowlatshahi D, MacQueen GM, Wang JF, Young LT. Increased hippocampal BDNF immunoreactivity in subjects treated with antidepressant medication. Biol Psychiatry 2001;50:260–5.
Duman RS, Monteggia LM. A neurotrophic model for stress-related mood disorders. Biol Psychiatry 2006;59:1116–27.
Dunham JS, Deakin JF, Miyajima F, Payton A, Toro CT. Expression of hippocampal brain-derived neurotrophic factor and its receptors in Stanley consortium brains. J Psychiatr Res 2009;43:1175–84.
Durany N, Michel T, Zochling R, Boissl KW, Cruz-Sanchez FF, Riederer P, et al. Brain-derived neurotrophic factor and neurotrophin 3 in schizophrenic psychoses. Schizophr Res 2001;52:79–86.
Eran A, Graham KR, Vataiaro K, McCarthy J, Collins C, Peters H, et al. Comment on "Autistic-like phenotypes in Cadps2-knockout mice and aberrant CADPS2 splicing in autistic patients". J Clin Invest 2009;119:679–80 author reply 680–671.
Girgenti, M. J., Nisenbaum, L. K., Bymaster, F., Terwilliger, R., Duman, R. S., Newton, S. S., Antipsychotic-induced gene regulation in multiple brain regions. J Neurochem 113, 175–187.
Hashimoto T, Bergen SE, Nguyen QL, Xu B, Monteggia LM, Pierri JN, et al. Relationship of brain-derived neurotrophic factor and its receptor TrkB to altered inhibitory prefrontal circuitry in schizophrenia. J Neurosci 2005;25:372–83.
Howes OD, Montgomery AJ, Asselin MC, Murray RM, Valli I, Tabraham P, et al. Elevated striatal dopamine function linked to prodromal signs of schizophrenia. Arch Gen Psychiatry 2009;66:13–20.
Iritani S, Niizato K, Nawa H, Ikeda K, Emson PC. Immunohistochemical study of brain-derived neurotrophic factor and its receptor, TrkB, in the hippocampal formation of schizophrenic brains. Prog Neuropsychopharmacol Biol Psychiatry 2003;27:801–7.
Krishnan V, Nestler EJ. The molecular neurobiology of depression. Nature 2008;455:894–902.
Liu Y, Schirra C, Stevens DR, Matti U, Speidel D, Hof D, et al. CAPS facilitates filling of the rapidly releasable pool of large dense-core vesicles. J Neurosci 2008;28:5594–601.
Lyon GJ, Abi-Dargham A, Moore H, Lieberman JA, Javitch JA, Sulzer D. Presynaptic regulation of dopamine transmission in schizophrenia. Schizophr Bull 2011;37:108–17.
Martinowich K, Manji H, Lu B. New insights into BDNF function in depression and anxiety. Nat Neurosci 2007;10:1089–93.
Mehler-Wex C, Grunblatt E, Zeiske S, Gille G, Rausch D, Warnke A, et al. Microarray analysis reveals distinct gene expression patterns in the mouse cortex following chronic neuroleptic and stimulant treatment: implications for body weight changes. J Neural Transm 2006;113:1383–93.
Nikolaus S, Antke C, Muller HW. In vivo imaging of synaptic function in the central nervous system: II. Mental and affective disorders. Behav Brain Res 2009;204:32–66.
Otsubo T, Miyaoka H, Kamijima K, editors. M.I.N.I. Mini international neuropsychiatric interview. Tokyo: Seiwa Shoten Publishers; 2005.
Sadakata T, Itakura M, Kozaki S, Sekine Y, Takahashi M, Furuichi T. Differential distributions of the Ca^{2+}-dependent activator protein for secretion family proteins (CAPS2 and CAPS1) in the mouse brain. J Comp Neurol 2006;495:735–53.
Sadakata T, Mizoguchi A, Sato Y, Katoh-Semba R, Fukuda M, Mikoshiba K, et al. The secretory granule-associated protein CAPS2 regulates neurotrophin release and cell survival. J Neurosci 2004;24:43–52.
Sadakata T, Kakegawa W, Mizoguchi A, Washida M, Katoh-Semba R, Shutoh F, et al. Impaired cerebellar development and function in mice lacking CAPS2, a protein involved in neurotrophin release. J Neurosci 2007a;27:2472–82.
Sadakata T, Washida M, Iwayama Y, Shoji S, Sato Y, Ohkura T, et al. Autistic-like phenotypes in Cadps2-knockout mice and aberrant CADPS2 splicing in autistic patients. J Clin Invest 2007b;117:931–43.

Please cite this article as: Hattori K, et al., Expression of Ca^{2+}-dependent activator protein for secretion 2 is increased in the brains of schizophrenic patients, Prog Neuro-Psychopharmacol Biol Psychiatry (2011), doi:10.1016/j.pnpbp.2011.05.004

Salio C, Lossi L, Ferrini F, Merighi A. Neuropeptides as synaptic transmitters. Cell Tissue Res 2006;326:583–98.
Sheehan DV, Lecrubier Y, Sheehan KH, Amorim P, Janavs J, Weiller E, et al. The Mini-International Neuropsychiatric Interview (M.I.N.I.): the development and validation of a structured diagnostic psychiatric interview for DSM-IV and ICD-10. J Clin Psychiatry 1998;59(Suppl. 20):22–33 quiz 34–57.
Siuciak JA, Lewis DR, Wiegand SJ, Lindsay RM. Antidepressant-like effect of brain-derived neurotrophic factor (BDNF). Pharmacol Biochem Behav 1997;56:131–7.
Takahashi M, Shirakawa O, Toyooka K, Kitamura N, Hashimoto T, Maeda K, et al. Abnormal expression of brain-derived neurotrophic factor and its receptor in the corticolimbic system of schizophrenic patients. Mol Psychiatry 2000;5:293–300.
Thomas EA. Molecular profiling of antipsychotic drug function: convergent mechanisms in the pathology and treatment of psychiatric disorders. Mol Neurobiol 2006;34:109–28.
Torrey EF, Webster M, Knable M, Johnston N, Yolken RH. The stanley foundation brain collection and neuropathology consortium. Schizophr Res 2000;44:151–5.
Weickert CS, Hyde TM, Lipska BK, Herman MM, Weinberger DR, Kleinman JE. Reduced brain-derived neurotrophic factor in prefrontal cortex of patients with schizophrenia. Mol Psychiatry 2003;8:592–610.

Please cite this article as: Hattori K, et al., Expression of Ca^{2+}-dependent activator protein for secretion 2 is increased in the brains of schizophrenic patients, Prog Neuro-Psychopharmacol Biol Psychiatry (2011), doi:10.1016/j.pnpbp.2011.05.004

EJN fens EUROPEAN JOURNAL OF NEUROSCIENCE

European Journal of Neuroscience, Vol. 31, pp. 1281–1291, 2010 doi:10.1111/j.1460-9568.2010.07164.x

BEHAVIORAL NEUROSCIENCE

Phenotypic characterization of a new *Grin1* mutant mouse generated by ENU mutagenesis

Tamio Furuse,[1] Yumiko Wada,[1] Kotaro Hattori,[2] Ikuko Yamada,[1] Tomoko Kushida,[1] Yoko Shibukawa,[1] Hiroshi Masuya,[3] Hideki Kaneda,[1] Ikuo Miura,[1] Naoki Seno,[4] Tomoyuki Kanda,[4] Ryo Hirose,[4] Shinichiro Toki,[4] Kousuke Nakanishi,[4] Kimio Kobayashi,[1] Hideki Sezutsu,[5,*] Yoichi Gondo,[5] Tetsuo Noda,[6] Shigeki Yuasa[2] and Shigeharu Wakana[1]

[1]Technology and Development Team for Mouse Phenotype Analysis: Japan Mouse Clinic, RIKEN Bioresource Center, 3-1-1 Koyadai, Tsukuba, Ibaraki 305-0074, Japan

[2]Department of Ultrastructural Research, National Institute of Neuroscience, National Center of Neurology and Psychiatry, Ogawa-Higashi, Kodaira, Tokyo, Japan

[3]Technology and Development Unit for Knowledge Base of Mouse Phenotype, RIKEN Bioresource Center, Koyadai, Tsukuba, Ibaraki, Japan

[4]Pharmaceutical Research Center, Kyowa Hakko Kogyo Co., Ltd., Shimotogari, Nagaizumi-cho, Sunto-gun, Shizuoka, Japan

[5]Mutagenesis and Genomics Team, RIKEN Bioresource Center, Koyadai, Tsukuba, Ibaraki, Japan

[6]Team for Advanced Development and Evaluation of Human Disease Models, RIKEN Bioresource Center, Koyadai, Tsukuba, Ibaraki, Japan

Keywords: animal model, behavior, D,L-methylphenidate, NMDA receptor

Abstract

In the RIKEN large-scale *N*-ethyl-*N*-nitrosourea (ENU) mutagenesis project we screened mice with a dominant mutation that exhibited abnormal behavior in the open-field test, passive avoidance test and home-cage activity test. We tested 2045 progeny of C57BL/6J males treated with ENU and untreated DBA/2J females in the open-field test and isolated behavioral mutant M100174, which exhibited a significant increase in spontaneous locomotor activity. We identified a missense mutation in the *Grin1* gene, which encodes NMDA receptor subunit 1, and designated the mutant gene $Grin1^{Rgsc174}$. This mutation results in an arginine to cysteine substitution in the C0 domain of the protein. Detailed analyses revealed that $Grin1^{Rgsc174}$ heterozygote exhibited increased novelty-seeking behavior and slight social isolation in comparison with the wild type. In contrast to other *Grin1* mutant mice, this mutant exhibited no evidence of heightened anxiety. These results indicate that this is a unique behavioral *Grin1* gene mutant mouse that differs from the known *Grin1* mutant mice. The results of immunohistochemical and biochemical analyses suggested that impaired interaction between the glutamatergic pathway and dopaminergic pathway may underlie the behavioral phenotypes of the $Grin1^{Rgsc174}$ mutant.

Introduction

N-ethyl-*N*-nitrosourea (ENU) is an effective chemical mutagen that introduces single base-pair changes into genomic DNA (Kohler *et al.*, 1991; Provost & Short, 1994). The point mutations that are induced by ENU can result in a large variety of aberrations ranging from complete or partial loss-of-function to gain-of-function. Several large-scale saturation ENU mutagenesis projects have been undertaken in order to generate large numbers of mutants that will allow gene functions to be systematically investigated *in vivo* (Justice *et al.*, 1999; Hrabe de Angelis *et al.*, 2000; Nolan *et al.*, 2000). The aim of our RIKEN mutagenesis project is to generate mouse models of human diseases, including diabetes, hypertension and cancer, and deformities. We have been screening dominant mutant mice for visible, clinical biochemical, and hematological abnormalities and have succeeded in establishing unique models of human disease (Inoue *et al.*, 2004; Masuya *et al.*, 2005, 2007). In 2007, Keays *et al.* (2007) reported finding that a mouse with ENU-induced mutation that exhibited hyperactivity in the open-field test and abnormal neuronal migration carried a missense mutation in alpha-tubulin (Tuba1a). The Tuba1a mutant mouse displayed phenotypic similarity to lissencephaly patients, and Keays *et al.* (2007) identified *de novo* mutations in *TUBA3*, the human homolog of Tuba1. As these findings indicated that ENU mutagenesis might be useful as a means of generating models of various psychiatric diseases, we have conducted behavioral screening that included the open-field test, passive avoidance test and home-cage activity test.

Correspondence: Dr S. Wakana, as above.
E-mail: swakana@brc.riken.jp

**Present address*: Transgenic Silkworm Research Center, National Institute of Agrobiological Sciences, 1-2 Owashi Tsukuba, Ibaraki 305-8634, Japan.

Received 11 May 2009, revised 2 February2010, accepted 3 February 2010

Materials and methods

Animals and production of ENU mutant mice

All animal studies were carried out in accordance with the guideline issued by the RIKEN Bioscience Technology Center in the 'Outline for conducting animal experiments' (August 1999, revised October 2001). The study was approved by the ethics committee of the RIKEN Tsukuba Institute. A large-scale mouse ENU mutagenesis was conducted as described previously (Masuya *et al.*, 2005) with some modifications. C57BL/6J (B6) and DBA/2J (D2) mice were purchased from a commercial supplier (CLEA Japan, Inc., Tokyo, Japan). The following outline strategy is given in more detail in Supporting information, Fig. S1. B6 males were treated with ENU (150–250 mg/kg) by intraperitoneal (i.p.) injection and crossed with D2 females. The progeny generated by this cross were designated G1 mice (supporting Fig. S1A). To obtain control data for genetic mapping and to confirm phenotypic transmission, D2 females and (D2 × B6) F1 mice were crossed. This cross yield D × DB mice (supporting Fig. S1B). G1 mice were then backcrossed with D2 mice six times for inheritance testing, gene mapping and elimination of other ENU-induced mutations (supporting Fig. S1C). In order to eliminate the effects of the D2 genetic background, an N6 mouse was backcrossed to B6 at least 10 times, and naive backcrossed progeny were used for all behavioral tests except the resident–intruder paradigm (supporting Fig. S1D). The F1 mice from the cross between N6 mice and B6 mice were used for the resident–intruder paradigm (supporting Fig. S1D). Male mice that had never undergone inheritance testing or linkage analysis were used in the behavioral tests in order to eliminate any influence of the female estrous cycle and previous handling.

Phenotype screening and gene mapping

We used locomotor activity in the open field as an index of abnormal behavior. The G1 mice were screened for abnormal open-field activity at 9 weeks of age. Mice that showed high or low activity (> mean ± 3 SD of the G1 population) were classified as behavioral phenodeviants and crossed with wild-type D2 mice to test for phenotypic transmission and genetic mapping. A total of 229 N2–6 mice (supporting Fig. S1C) between 10 and 12 weeks of age were collected and tested for spontaneous locomotor activity in the open field. A genome-wide scan was conducted as described previously (Masuya *et al.*, 2005) with some modifications. Single nucleotide polymorphism (SNP) markers spaced at 10 cm were chosen from the Mouse SNP database (http://www.broad.mit.edu/snp/mouse/) and used for genome-wide scanning (supporting Table S1). We used microsatellite or SNP markers for a detailed linkage analysis. Candidates for the causative gene located near the mapped locus were identified by searching the positional cloning assistant database Positional MEDLINE (PosMed, http://omicspace.riken.jp/PosMed/; Kobayashi & Toyoda, 2008). The genomic structures of the candidates were determined with the mouse Ensembl database (http://www.ensembl.org/Mus_musculus/index.html), and coding regions were directly sequenced. The accession numbers of all of these genes are listed in Table 1.

TABLE 1. List of candidate causative genes

Gene name	No. of exons sequenced	No. of exons	MGI accession no.
Hnmt	7	7	2153181
Cacna1b	47	48	88296
Ehmt1	23	26	1924933
Arrdc1	7	8	2446136
Zmynd19	5	6	1914437
NM_026044	9	9	1914478
Q9CQN7	2	2	1333816
Nelf	14	15	1861755
Entpd8	10	10	1919340
Noxa1	6	12	2449980
NM_026624	7	7	3605773
Grin1	18	20	95819
Npdc1	8	9	1099802
Clic3	6	7	1916704
Ptgds	6	7	99261

Candidate genes for the mutant line from founder mouse M100174 obtained by a search of the PosMed database are listed. Accession numbers of genes used for primer design are listed on the right side of the table. MGI, Mouse Genome Informatics (http://www.informatics.jax.org/). The genomic sequences and exon/intron structures of each gene were retrieved from the Ensembl Mouse database (http://www.ensembl.org/Mus_musculus/index.html) by entering MGI accession numbers. Sequencing of 191 of the 210 exons in these 18 genes was performed.

Mutation analysis of the Grin1 gene

The C-to-T point mutation in exon 18 of *Grin1* was identified by using the allele-specific primer–polymerase chain reaction (ASP-PCR) and direct sequencing. ASP-PCR was performed with the following primers: forward primer for wild-type and mutant alleles, tgctgagggtccctcacag; reverse primer for the wild-type allele, agctgcatctgcttcctagg; reverse primer for the mutant-type allele, agctgcatctgcttcctaga.

Homology search and accession number of the amino acid sequence

The accession number of the amino acid sequence used for alignment was A2AI21.

Open-field test

Each mouse was placed in the corner of an open-field apparatus (400 wide × 400 long × 300 high; O'Hara & Co., Ltd., Tokyo, Japan) made of white polyvinyl chloride. The distance traveled by each animal in the open field was recorded for 20 min with a video imaging system (Image OF9; O'Hara & Co., Ltd.).

Home-cage activity test

Each mouse was placed alone in a testing cage (227 × 329 × 133 mm) under a 12-h light–dark cycle (light on at 08:00 h) and had free access to both food and water. After 1 day of acclimation, spontaneous activity in the cage was measured for 5 days (starting at 08.00) with an infrared sensor (AB system 4.0; Neuroscience Co., Ltd., Tokyo, Japan).

Object exploration test

We used the procedure described previously (Glenn *et al.*, 2008; Tomihara *et al.*, 2009) with some modifications. Each mouse was placed in the open-field apparatus without the novel object for 20 min of acclimation before testing. A transparent acrylic tube (bottom diameter, 66 mm; top diameter, 44 mm; height, 154 mm) containing marbles was placed in the center of the open field. The total time spent exploring the object and the frequency of exploration during a 10-min period were determined with a video imaging system purchased from a commercial supplier (O'Hara & Co., Ltd.). Exploration was defined as the state when the distance between the object and the mouse was < 1 cm.

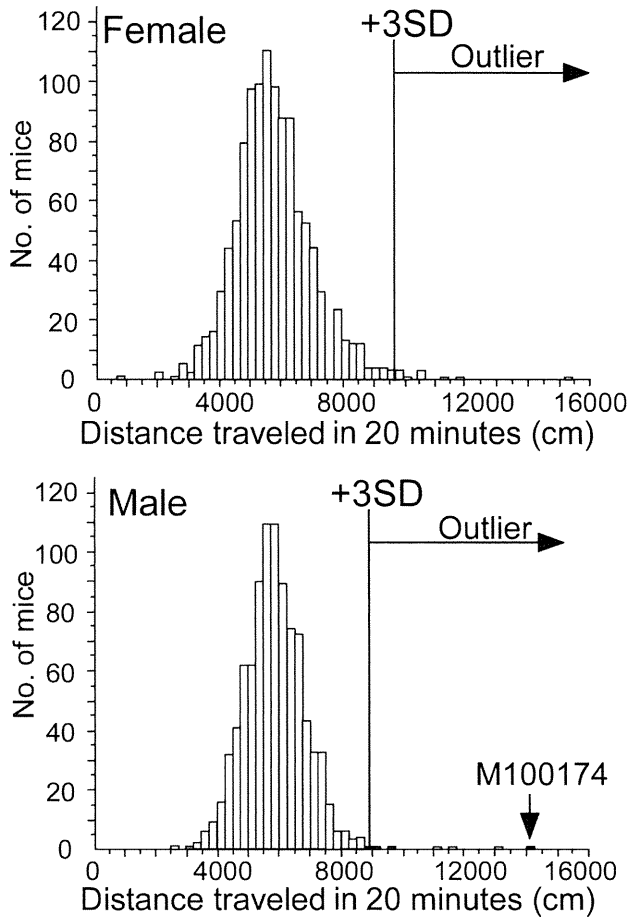

FIG. 1. Histograms of the open-field activity of G1 mice. The ordinate and abscissa indicate the number of mice and the distance traveled, respectively. The vertical line in the histograms indicates the population > 3 SD above the mean. Spontaneous activity during the open-field test was normally distributed. Mice whose activity level was > 3 SD above the mean (the mean was 9734.9 cm for G1 females and 8984.9 cm for G1 males) were isolated as mutant candidates. The vertical arrow indicates the activity level of the M100174 mouse.

Effect of D,L-methylphenidate hydrochloride (MPH) on spontaneous locomotor activity in the open-field

Each mouse was acclimated to the open field as above described for 1 h. Mice were injected intraperitoneally with saline or a 30 mg/kg dose of MPH (SIGMA-ALDRICH, St. Louis, MO, USA). The free base of methylphenidate was calculated as 108 μmol/kg dose. Locomotor activity in the open-field apparatus was measured as described above for 20 min, beginning at 80 min after the injection (Gainetdinov *et al.*, 1999). To assess the dose- and time-dependence of the effect of MPH, small pilot experiments were carried out in which various doses were given (supporting Appendix S1 and Fig. S2).

Measurement of NMDA-induced changes in intracellular calcium levels in mouse primary cortical neurons

Dissociated cerebral cortical cells were prepared from embryonic day (E) 14–15 mice as described in supporting Appendix S2. Pregnant female mice were killed by cervical-vertebrae dislocation and isolated embryos were killed by decapitation before removing the brain. The cells were stimulated with 10 μM *N*-methyl-D-aspartate (NMDA) and 100 μM glycine at 37°C, and fluorescence (excitation wavelength, 480 nm; emission wavelength, 540 nm) was measured with an FDSS6000 fluorimeter (Hamamatsu Photonics, Hamamatsu, Japan).

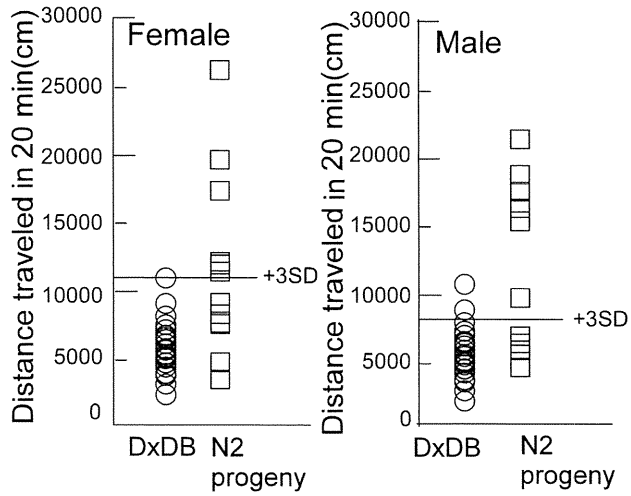

FIG. 2. Distribution of the locomotor activity of the N2 progeny of the M100174 founder mouse and the control mice (D × DB). Locomotor activity of D × DB (females, n = 68; males, n = 74) and the N2 progeny of M100174 (females, n = 12; males, n = 10) in the open-field test. Open circles, D × DB; open squares, N2 progeny of M100174. The horizontal line indicates the locomotor activity criterion that divides wild-type mice and mutant mice (3 SD above the mean in the D × DB population).

Immunoblotting of NMDA receptor (NMDAR) subunits

The brain tissue samples were prepared as described previously (Bajo *et al.*, 2006) with a slight modification (supporting Appendix S3). Mice were killed by cervical-vertebra dislocation. The blotted membranes were blocked with Starting Block TBS-T (Pierce, Rockford, IL, USA) for 10 min and probed with the following primary antibodies: mouse antineuronal class III β-tubulin (Covance, Berkeley, CA, USA) and rabbit anti-*GRIN1*, anti-GRIN2A and anti-GRIN2B (Frontier Science Ishikari, Hokkaido, Japan). After washing three times with Tris-buffered saline (TBS; pH 7.5) containing 0.1% Tween 20 (TBS-T), the membranes were incubated with horseradish peroxidase-labeled secondary antibody, and signals were detected with SuperSignal West Femto (Pierce) and LAS1000 mini (Fujifilm, Tokyo, Japan).

Immunoblotting of extracellular signal-regulated kinase (ERK2) and phospho-ERK2 (pERK2) proteins

At 90 min after i.p. injection of saline or MPH 30 mg/kg, the nucleus accumbens was prepared as reported previously (Hattori *et al.*, 2006; supporting Appendix S4). Mice were killed by cervical-vertebra dislocation. The proteins were transferred onto membranes, and ERK proteins were probed and signals detected as described above [primary antibodies, 1 : 50 000 dilution for anti-pERK antibody and 1 : 20 000 for anti-ERK antibody (Cell Signaling Technology, Danvers, MA, USA), horseradish peroxidase-labeled secondary antibody and anti-rabbit IgGs, 1 : 5000 dilution for pERK and 1 : 2000 dilution for ERK (Pierce)].

General histology and Nissl staining

Mice were deeply anesthetized by i.p. pentobarbital injection and then fixed by transcardiac perfusion with a solution of 4%

paraformaldehyde and 0.5% picric acid in PBS. The brains were removed, and coronal or parasagittal sections (70 μm thick) were prepared with a vibratome. Sections were stained with NeuroTrace 500/525 (fluorescent Nissl stain; Invitrogen, Carlsbad, CA, USA) according to the manufacturer's instructions. Fluorescence images were obtained directly with a confocal laser-scanning microscope (LSM5 Pascal; Zeiss, Oberkochen, Germany).

Immunohistological study of c-Fos expression

Two hours after i.p. injection of saline or MPH 30 mg/kg, mouse brains were perfusion-fixed and removed, and sections were prepared as described above. The sections were postfixed in the same fixative for 2 h at 4–8°C and then rinsed with PBS. c-Fos immunostaining and quantification of c-Fos-positive neurons were performed as reported previously (Hattori *et al.*, 2001). Brain regions that were responsive to MPH treatment were selected as described in the literature (Yano & Steiner, 2005).

Statistical analysis

Two-way (genotype and experimental factor: between-subjects) or three-way (genotype, sex, and experimental factor: between- or within-subjects) ANOVA with Fisher's PLSD *post hoc* analysis and Student's *t*-test were used for statistical analysis. Differences were considered to be statistically significant at *P*-values < 0.05.

Results

Isolation of a mutant with increased locomotor activity and identification of a missense mutation in the Grin1 gene

We used the total distance traveled during the open-field test to screen locomotor activity in a population of 2045 (female, n = 1124; male, n = 921) G1 mice in a large-scale ENU mutagenesis program conducted at the RIKEN Genome Science Center. Mouse M100174 exhibited the highest locomotor activity among the male G1 population (Fig. 1), and this founder mouse was backcrossed with D2 females, and 22 offspring of the backcrossed mice (N2 progeny)

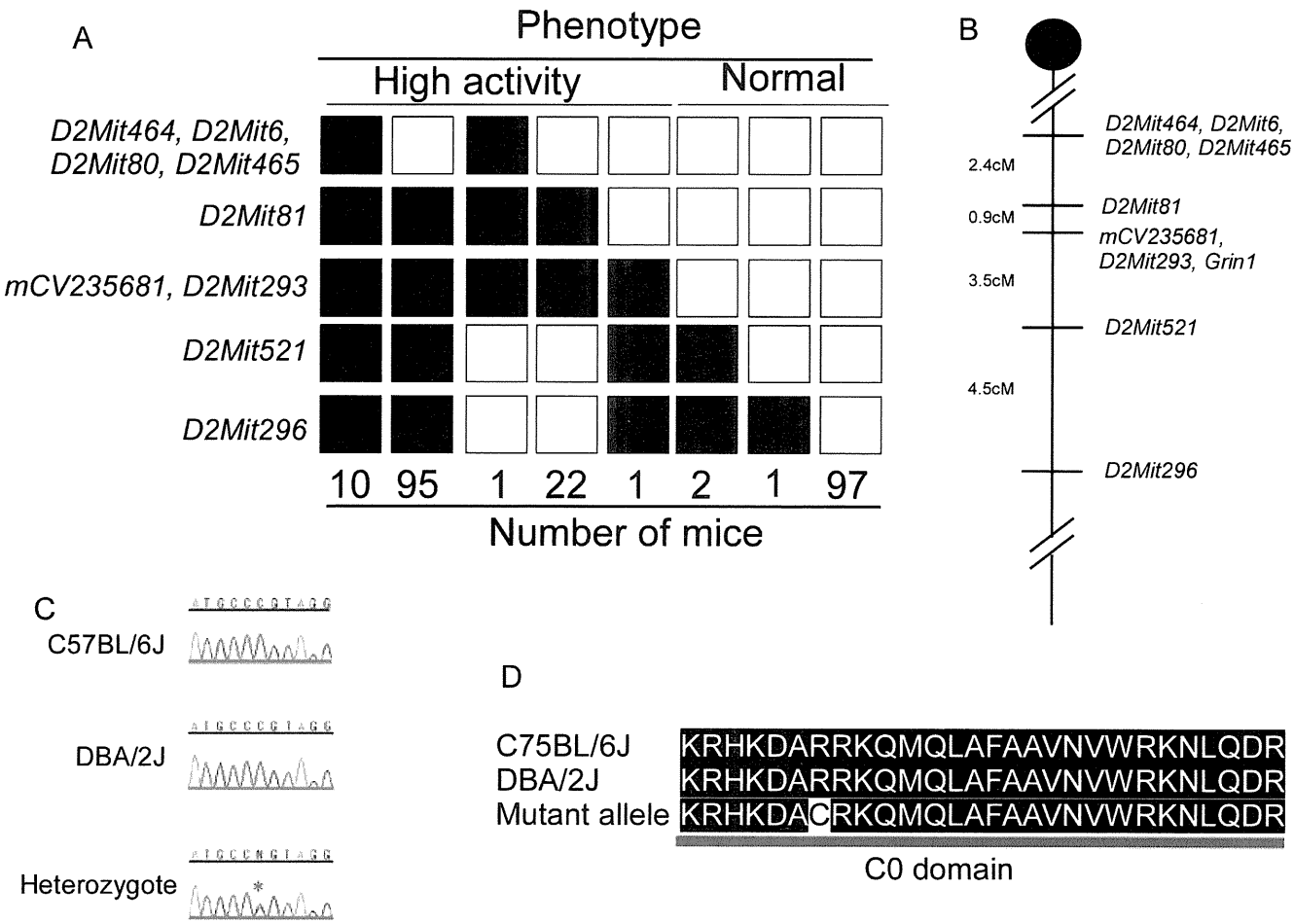

FIG. 3. Mutant mouse line M100174 carries a missense mutation in *Grin1*, which encodes NMDAR1. (A) Haplotype analysis of backcrossed progeny of M100174. Genetic markers are listed on the left side of the panel. The black boxes represent the heterozygote of C57BL/6J and DBA/2J, and the white boxes represent the homozygote of DBA/2J. The numbers of progeny that inherited each haplotype are shown at the bottom. (B) Genetic map of M100174 constructed from the backcrossed progeny of G1 mice. Genetic markers are listed on the right. (C) Sequence trace from a heterozygote. The C-to-T substitution is highlighted with an asterisk and corresponds to a point mutation in exon 18 of *Grin1*. (D) Alignment of the C0 domain of wild-type NMDAR1 with that of the mutant allele. Conserved amino acids sequences are highlighted in black. The C-to-T mutation results in an amino acid substitution in the C0 domain of NMDAR1.

TABLE 2. Numbers and percentages of wild-type, heterozygous and homozygous pups obtained by intercrossing heterozygote

	Grin1 gene genotype: number of pups (and %)				
Age	Wild	Hetero	Homo	Total	Genetic background
E14	15 (22)	34 (50)	19 (28)	68 (100)	N9 × N9
E17–18	25 (41)	28 (46)	8 (13)	61 (100)	N10 × N10
P4w	11 (35)	19 (62)	1 (3)	31 (100)	N5 × N5

Pups were generated by mating heterozygous females and males. The parents of the pups were generated by backcrossing M100174 with DBA/2J or C57BL/6J. The genetic background of the parents is indicated by the backcross generation. The proportions of offspring according to genotypes were examined at embryonic day 14 (E14), embryonic day 17–18 (E17–18), and 4 weeks after birth (P4w). Wild, +/+; Hetero, $Grin1^{Rgsc174}$/+; Homo, $Grin1^{Rgsc174}/Grin1^{Rgsc174}$.

were generated for the inheritance test. Based on their level of open-field activity the N2 progeny were divided into a normal group and an increased locomotion group by scoring the animals relative to the mean open-field activity of D × DB mice (Fig. 2). A total of 229 mice from generations N2–N6 were collected and used for a linkage analysis. The causative locus was mapped to a region between D2Mit81 and D2Mit521 (Fig. 3A and B).

A search of the Ensembl mouse genome database revealed that 172 genes were located between D2Mit81 and D2Mit521, and these candidates were investigated with PosMed. Based on a list of keywords related to behavior, PosMed narrowed the number down to 18 candidate genes (Table 1), and one of them, *Grin1* (glutamate receptor, ionotropic, NMDA1), was a strong candidate. *Grin1* encodes NMDAR1 protein, and analysis of the *Grin1* sequence revealed a C-to-T mutation in exon 18 of the gene (Fig. 3C). This mutation results in a substitution of arginine for cysteine at residue 844. We designated the *Grin1* mutant allele $Grin1^{Rgsc174}$ (where 'Rgsc' indicates RIKEN Genome Science Center).

$Grin1^{Rgsc174}$ homozygotes exhibited perinatal lethality, but heterozygotes were histologically normal

$Grin1^{Rgsc174}$ heterozygotes of both sexes mated naturally and were fertile. At E14, wild-type, heterozygous ($Grin1^{Rgsc174}$/+) and homozygous ($Grin1^{Rgsc174}/Grin1^{Rgsc174}$) fetuses were present in the uterus. The number of homozygous pups gradually decreased from E17/E18 to 4 weeks postnatally (Table 2). No obvious morphological defects were detected in Nissl-stained tissue sections of the brains of the heterozygote ($Grin1^{Rgsc174}$/+; supporting Fig. S3).

Altered NMDAR function in $Grin1^{Rgsc174}$ heterozygote without any reduction in GRIN protein expression

To investigate the effect of the $Grin1^{Rgsc174}$ allele on NMDAR function, primary cultured cortical neurons were prepared from homozygous, heterozygous and wild-type pups, and transient calcium influx was measured by fluorescence imaging after 10 μM NMDA stimulation. ANOVA showed a significant effect of genotype on the maximum calcium influx after NMDA stimulation and on its duration at half-maximal calcium levels ($T_{1/2max}$). The maximum calcium influx level in the homozygote was significantly higher than in the wild type (Fig. 4A), and $T_{1/2max}$ was significantly longer in the homozygote than in either the wild type or the heterozygote (Fig. 4B). GRIN1, GRIN2A and GRIN2B protein levels were determined in the adult cingulate cortex by immunoblotting, but no differences were found between the heterozygous and wild-type mice (Fig. 5A and B).

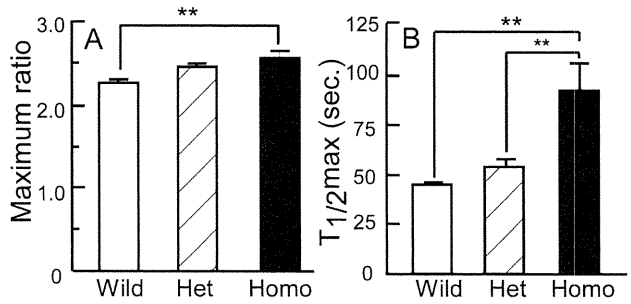

FIG. 4. Fluorescence imaging of transient NMDA-induced calcium influxes in primary cultured cortical neurons from E14 mouse embryos. (A) Maximum calcium influx after stimulation with 10 μM NMDA relative to baseline intracellular calcium levels. ANOVA, effect of genotype, $F_{2,32} = 5.4$, $P < 0.013$. $^{**}P < 0.004$, Fisher's PLSD. (B) Duration at half-maximal calcium level ($T_{1/2max}$) after 10 μM NMDA. ANOVA, effect of genotype, $F_{2,32} = 8.4$, $P < 0.002$; $^{**}P < 0.01$, Fisher's PLSD. White columns, wild type; hatched columns, $Grin1^{Rgsc174}$/+; black columns, $Grin1^{Rgsc174}/Grin1^{Rgsc174}$. Error bars represent the SEM; $n = 5$ of each genotype.

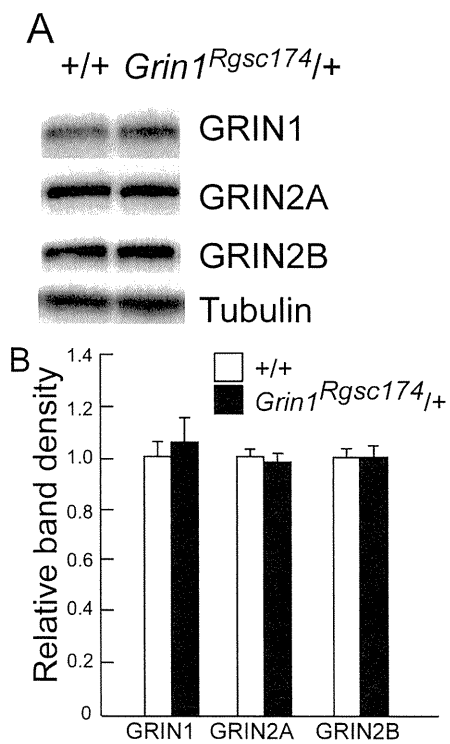

FIG. 5. Expression of NMDAR subunits in the cerebral cortex of wild-type and $Grin1^{Rgsc174}$/+ mice. (A) Protein fractions prepared from the cerebral cortex of adult +/+ and $Grin1^{Rgsc174}$/+ mice were subjected to immunoblotting. A representative immunoblot for GRIN1, GRIN2A and GRIN2B NMDAR subunits and an internal control (neuronal class III β-Tubulin) is shown. (B) Quantification of NMDAR subunit expression. The average expression level of each subunit relative to tubulin (neuronal class III β-Tubulin) is shown. There were no significant differences between the levels of expression in $Grin1^{Rgsc174}$/+ and +/+ mice. Error bars represent the SEM. Male mice, $n = 5$ of each genotype. Student's *t*-test, *GRIN1*: $t_8 = 0.652$, $P > 0.5$; GRIN2A: $t_8 = -0.678$, $P > 0.5$; GRIN2B: $t_8 = -0.244$, $P > 0.8$.

Behavioral abnormalities of $Grin1^{Rgsc174}$ mice

$Grin1^{Rgsc174}$ heterozygotes exhibited increased locomotor activity in the open-field test (Fig. 6A), and $Grin1^{Rgsc174}$/+ mice displayed increased locomotor activity in their familiar home cage (Fig. 7A) as a

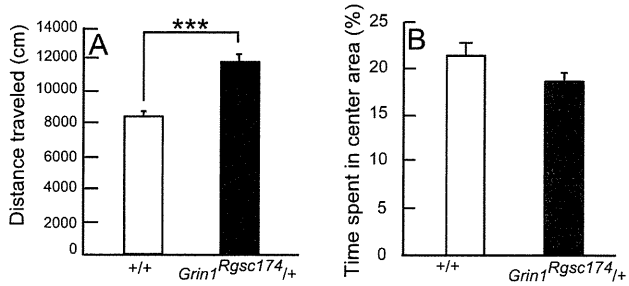

FIG. 6. Locomotor activity of +/+ and *Grin1*^{Rgsc174}/+ mice in the open-field test. (A) Distance traveled in the open field during a 20-min period. Student's *t*-test, $t_{18} = -6.3$, ***$P < 0.0001$. (B) Time spent in the center (30% of the open-field arena). Student's *t*-test, $t_{18} = 1.9$, $P > 0.6$. Error bars represent the SEM. Male mice, $n = 10$ in each group at 8 weeks of age.

result of an increase during the dark period (Fig. 7B and C). The heterozygote exhibited normal rest–activity cycles in their home cage under a standard light–dark cycle (Fig. 7D).

The novelty-seeking behavior of heterozygote was assessed by measuring time spent exploring a novel object placed in the center of the open field. *Grin1*^{Rgsc174}/+ mice spent a longer time exploring the tube filled with marbles than did the wild-type mice (Fig. 8A), and they also explored the tube more frequently (Fig. 8B). However, the time spent in exploring the object by the heterozygous and wild-type mice during each visit (mean duration) was almost the same (Fig. 8C).

In the social interaction test (supporting Appendix S5), the frequency of interaction with another subject of same genotype by heterozygote was similar to that of the wild type (supporting Fig. S4A) but, as the heterozygote spent a shorter time during each interaction with the other subject (supporting Fig. S4B), the total interaction time with the other subject in the open-field area was shorter than it was for the wild type (supporting Fig. S4C). In the resident–intruder paradigm (supporting Appendix S6), the numbers of resident heterozygous mice and wild-type mice that attacked the intruder, either by mounting or biting, were similar (supporting Table S2). Heterozygotes did not display increased anxiety in the light–dark transition test (supporting Appendix S7 and Fig. S5), and

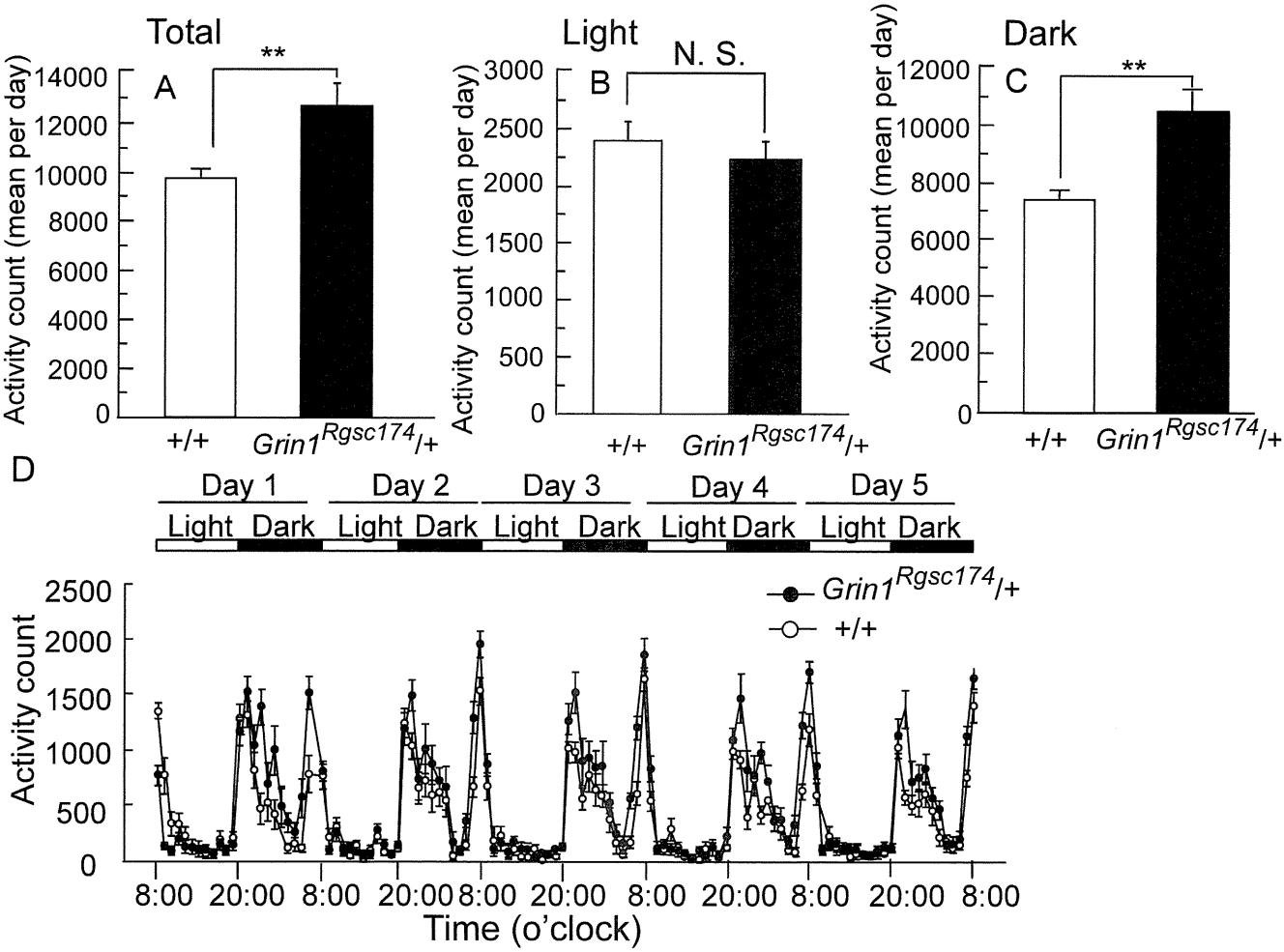

FIG. 7. Locomotor activity of +/+ and *Grin1*^{Rgsc174}/+ mice in their home cages. (A) Mean daily locomotor activity in the home cage. Student's *t*-test, $t_{18} = -3.3$, **$P < 0.01$. (B) Mean locomotor activity in the home cage during the light period. N.S. indicates no significant difference between the two groups, Student's *t*-test, $t_{18} = 0.68$, $P > 0.5$. (C) Mean locomotor activity in the home cage during the dark period. Student's *t*-test, $t_{18} = -0.39$, **$P < 0.01$. (D) Locomotor activity patterns of +/+ and *Grin1*^{Rgsc174}/+ mice during the light/dark cycle. ANOVA, effect of genotype, $F_{1,18} = 15.51$, $P < 0.003$. Error bars represent the SEM. Male mice, $n = 10$ of each genotype at 10–12 weeks of age.

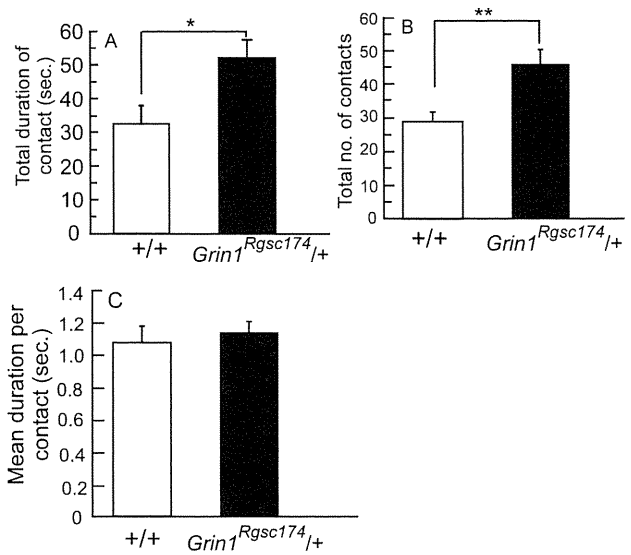

FIG. 8. Object exploration by *Grin1*^{Rgsc174}/+ and wild-type mice. (A) Total time *Grin1*^{Rgsc174}/+ and +/+ mice spent exploring the object. Student's *t*-test, $t_{18} = 2.7$, $^{*}P < 0.05$. (B) The total number of times *Grin1*^{Rgsc174}/+ and +/+ mice made contact with the novel object. Student's *t*-test, $t_{18} = -3.1$, $^{**}P < 0.001$. (C) Duration of each exploration by *Grin1*^{Rgsc174}/+ and +/+ mice. Student's *t*-test, $t_{18} = 0.6$, $P > 0.5$. Error bars represent the SEM. Male mice, $n = 10$ of each genotype at 11 weeks of age.

no significant difference was observed in the time spent in the center area of the open field (Student's *t*-test, $t_{18} = 1.9$, $P > 0.069$; Fig. 6B).

Pharmacological analysis with MPH

A significant interaction effect between genotype and drug treatment was detected in the open-field test (ANOVA, $F_{1,836} = 210.549$, $P < 0.0001$). Wild-type mice displayed increased locomotor activity following administration of MPH 30 mg/kg (Fig. 9A; Fisher's PLSD, $P < 0.0001$), whereas a sustained reduction in locomotor activity was observed in *Grin1*^{Rgsc174}/+ mice following MPH administration (Fig. 9B; Fisher's PLSD, $P < 0.0001$).

To determine how MPH alters neuronal activity, we immunohistochemically examined the expression of an immediate–early gene, c-Fos, in the brain and plotted (Fig. 10A) the c-Fos-immunoreactive (IR) cells onto a brain atlas (Paxinos & Franklin, 1997). The heterozygote exhibited a characteristic phenotype in the dorsal striatum and prelimbic cortex. In the wild type, the number of c-Fos-IR-cells significantly increased in the dorsal striatum, following MPH administration (Fig. 10Aa and Ab; supporting Fig. S6Aa and Ab), whereas the number increased to a lesser degree in the heterozygote (Fig. 10Ac and Ad; supporting Fig. S6Ac and Ad). On the other hand, although the number of c-Fos-IR cells in the prelimbic cortex of the wild type increased significantly following MPH administration (Fig. 10Aa and Ab; supporting Fig. S6Aa and Ab), the basal level of c-Fos-IR cells was much higher in the prelimbic cortex of the heterozygote and the number of c-Fos-IR cells in the prelimbic cortex were decreased following MPH administration (Fig. 10Ac and Ad; supporting Fig. S6Ac and Ad). To identify the MPH-responsive neurons we stained for c-Fos immunoreactivity and counterstained with Nissl reagent, and the results showed that c-Fos was mainly expressed in the pyramidal cells of the prelimbic cortex (supporting Fig. S6Be and Bf).

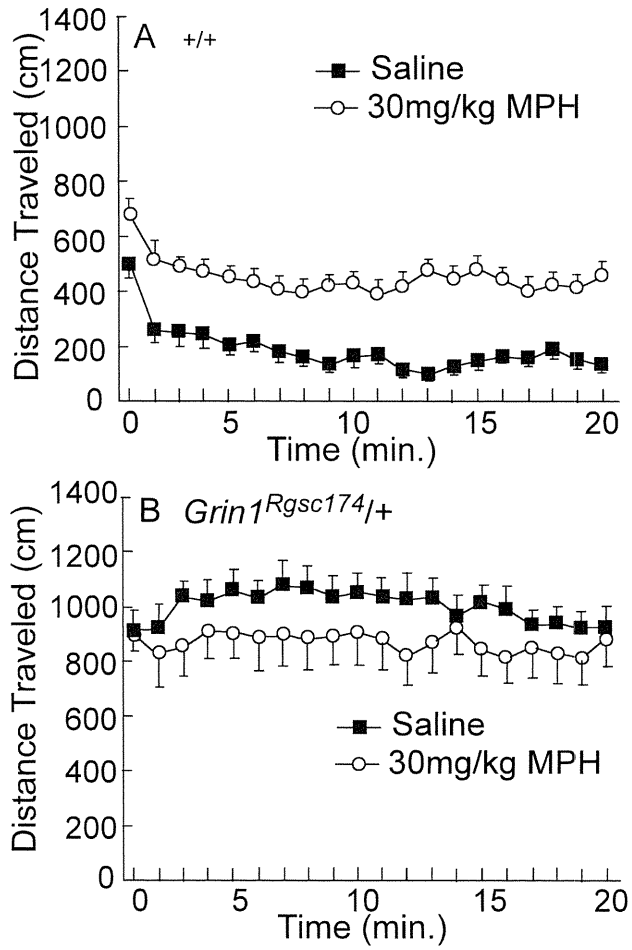

FIG. 9. Effect of MPH on the locomotor activity of *Grin1*^{Rgsc174}/+ and +/+ mice. The distance traveled by (A) wild-type and (B) *Grin1*^{Rgsc174}/+ mice in the open field 80 min after saline or MPH injection. Error bars represent the SEM. Male mice, $n = 10$ of each genotype at 11 weeks of age.

Significant effects of genotype, MPH treatment, and interaction between genotype and MPH treatment were detected in the dorsal striatum (Fig. 10B). The basal levels of c-Fos expression in the wild type and heterozygote were similar. MPH treatment increased c-Fos expression in both the wild-type and heterozygous mice. c-Fos expression in the dorsal striatum of the MPH-treated heterozygote was lower than in the MPH-treated wild type. There was a significant effect of genotype and MPH treatment on c-Fos expression in the prelimbic cortex (Fig. 10C), and a significant interaction between genotype and MPH treatment was also detected. More c-Fos-IR cells were present in the prelimbic cortex of saline-treated heterozygotes than of the wild type. MPH treatment significantly increased c-Fos expression in the wild-type prelimbic cortex but suppressed c-Fos expression in the prelimbic cortex of the heterozygote.

In the nucleus accumbens, there was a significant effect of MPH administration and a significant interaction between the MPH effect and genotype on the pERK2 level (Fig. 11). Fisher's PLSD test was used to clarify the rank relationship between the baseline group and other groups statistically. The pERK2 level in the nucleus accumbens of the MPH-treated wild type was significantly greater than baseline level. The baseline pERK level in the heterozygote was higher than in the wild type, but the pERK2 level in the MPH-treated heterozygote